Wavelet Domain Communication System (WDCS): Design, Model, Simulation, and Analysis

Randall W. Klein

Recommended Citation

Klein, Randall W., "Wavelet Domain Communication System (WDCS): Design, Model, Simulation, and Analysis" (2001). *Theses and Dissertations*. 4647.
https://scholar.afit.edu/etd/4647

WAVELET DOMAIN COMMUNICATION SYSTEM (WDCS):

DESIGN, MODEL, SIMULATION, AND ANALYSIS

THESIS

Randall W. Klein, Second Lieutenant, USAF

AFIT/GE/ENG/01M-16

DEPARTMENT OF THE AIR FORCE
AIR UNIVERSITY

AIR FORCE INSTITUTE OF TECHNOLOGY

Wright-Patterson Air Force Base, Ohio

20010706 171

The views expressed in this thesis are those of the authors and do not reflect the official policy or position of the United States Air Force, Department of Defense or the U.S. Government.

WAVELET DOMAIN COMMUNICATION SYSTEM (WDCS):

DESIGN, MODEL, SIMULATION, AND ANALYSIS

THESIS

Presented to the Faculty

Department of Electrical and Computer Engineering

Graduate School of Engineering and Management

Air Force Institute of Technology

Air University

Air Education and Training Command

In Partial Fulfillment of the Requirements for the

Degree of Master of Science in Electrical Engineering
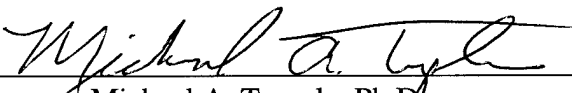
Randall W. Klein, B.S.E.E

Second Lieutenant, USAF

March 2001

WAVELET DOMAIN COMMUNICATION SYSTEM (WDCS):

DESIGN, MODEL, SIMULATION, AND ANALYSIS
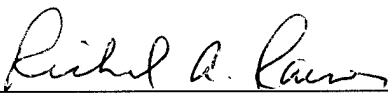
Randall W. Klein, B.S.E.E
Second Lieutenant, USAF

Approved:
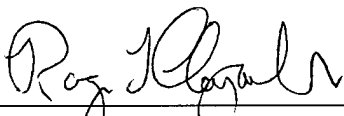
_____   _____
Michael A. Temple, Ph.D.   Date
Committee Chairman
5 Mar 01

_____   _____
Richard A. Raines, Ph.D., Major, USAF   Date
Committee Member
5 Mar 01

_____   _____
Roger L. Claypoole, Ph.D., Major, USAF   Date
Committee Member
5 MAR 01

ACKNOWLEDGMENTS

TABLE OF CONTENTS

TABLE OF FIGURES

ABSTRACT

A proposed wavelet domain communication system (WDCS) using transform domain processing is demonstrated as having enhanced interference avoidance capability under adverse environmental conditions. The WDCS system samples the environment and uses the wavelet transform, to determine interference presence and time/scale location. A digital communication waveform (basis function) is subsequently designed in the wavelet domain to specifically avoid regions containing interference. The WDCS basis function is data modulated prior to transmission. Assuming perfect synchronization, the receiver replicates a locally generated basis function for correlating with the received signal and demodulating the data. The proposed system is modeled and simulation results are obtained using MATLAB®. Bit error rate is the metric for analysis and performance comparisons. Relative to an equivalent DSSS, the WDCS provided bit error performance improvement in several different interference scenarios. The system also demonstrated comparable performance to a developmental TDCS while providing significant improvement in scenarios containing swept-tone interference. The system was evaluated using a signal bit energy-to-noise power level (E_b/N_o) of 4.0 dB and interference energy-to-signal energy (I/E) ratios ranging from 0 dB to 16.0 dB. As defined, performance improvement metrics representing the ratio of DSSS-to-WDCS and DSSS-to-TDCS bit error rates were used for characterizing performance. For antipodal data modulation, the average (over all interference scenarios) DSSS-to-WDCS performance improvement was 12.4 dB, approximately equal to the DSSS-to-TDCS (comparable performance). For binary orthogonal data modulation, the average DSSS-to-WDCS improvement was 5.7 dB vs. 6.8 dB for the DSSS-to-TDCS comparison. These results indicate the proposed WDCS is a viable option for interference avoidance communications and worthy of further study.

Wavelet Domain Communication System (WDCS):
Design, Model, Simulation, and Analysis

CHAPTER 1
INTRODUCTION

1.1 Background

Reliable communication is a concern in both the military and commercial world. Reliable is a subjective term, but with respect to digital communications, a system fails to be reliable when too many bits are received in error. Communication channel interference is a major contributor to increased bit error. Such interference can be classified as either intentional or unintentional. With most military communication systems, the ability to operate in the presence of intentional interference (jamming) is a necessity; much communications research is now directed towards securing such ability. One developmental system that has demonstrated interference avoidance capability is the transform domain communication system (TDCS) [8]. The TDCS is designed to successfully operate in the presence of both intentional and unintentional interference.

One source of unintentional interference is additive white Gaussian noise (AWGN), i.e., noise having a constant power spectral density (PSD) over all frequencies. Other sources of unintentional interference include other systems operating within, or producing harmonic energy within, the spectral region of interest, e.g., radio stations, television stations, cellular communications, navigational aids/transponders, airport radar, etc. Intentional interference (jamming) is an energy source specifically directed at the communication system with the intent of disrupting (perhaps completely) effective operation; such interference is primarily associated with military applications. Interference may be classified as narrowband or wideband depending

1

on the amount of bandwidth, with respect to the system's bandwidth, occupied by the interference. Narrowband interference exists at frequencies entirely within the system's operational bandwidth. Within the narrowband classification, there are four subcategories: single-tone, multiple-tone, swept-tone, and partial-band. Single tone interference has energy at one frequency (ideally) and if properly located, it can be the most disruptive. Multiple-tone interference consists of several, single frequency tones dispersed throughout the system bandwidth. Although multiple-tone interference covers more frequencies, given a finite amount of available jammer energy (power), each tone contains less energy per frequency. Swept-tone interference is manifest as single-tone that changes frequency with respect to time, losing time-stationary characteristics that will be discussed later. Partial-band interference contains energy over a continuous range of frequencies (typically covering a fractional portion of the system bandwidth). Interference energy can spread equally over a continuous range of frequencies, perhaps extending beyond the system's bandwidth, in which case the system noise floor is effectively raised. Between the two classifications, narrowband interference is generally more prevalent and easier to generate if intentional interference (jamming) is the goal. For this reason, most current research is directed toward mitigating narrowband-interference effects.

There are many different digital communication modulation schemes in use with the traditional methods including phase-, frequency-, and amplitude-shift keying. Despite differences between the modulation schemes, the transmitted signals share similar spectral characteristics, i.e., approximately 90% of the signal power is contained in a spectral region equaling twice the symbol transmission rate (null-to-null bandwidth). Excluding traditional spread spectrum techniques, the transmitted signal energy is typically well above the system noise floor level. Although necessary for reliable symbol demodulation and subsequent bit

2

estimation, this positive signal-to-noise ratio (SNR) condition allows unintended receivers to easily detect communication system operation. Once detected, it is easy to intentionally generate interference at the correct spectral location and disrupt system operation.

Traditional spread spectrum techniques represent a significant development in digital communications. Direct sequence spread spectrum (DSSS) systems have the inherent ability to effectively suppress the adverse affects of both unintentional and intentional interference. Functionally, a DSSS system works by 1) spreading the desired communication symbol energy beyond its original bandwidth, 2) transmitting the spread waveform, and then 3) despreading (focusing) the original symbol energy at the receiver. While despreading the desired waveform, the incident interfering energy is simultaneously spread – a portion of the original interference energy, originally falling within the system bandwidth, now falls outside and is suppressed by subsequent filtering. Therefore, the despreading and filtering operation effectively lowers the interference energy level relative to the desired signal energy and results in better (lower) bit error performance. The original DSSS bandwidth spreading typically results in a negative SNR condition, which makes it more difficult for an unintended receiver to detect the signal; thus, a DSSS system is characterized as providing a low probability-of-intercept (LPI) capability [6]. Even though the DSSS technique effectively lowers interference levels, sufficient interference energy remains to cause degradation.

Until the 1980's, both transmitter and receiver used time-domain signal-processing techniques to mitigate interference. The transmitter generated a shaped, time-domain waveform to achieve desired performance. The receiver subsequently used time-domain signal processing techniques, e.g., matched filtering or correlation, to demodulate the signal. In this case, both transmitter and receiver accepted the signal's resultant frequency domain representation.

3

In 1978, Milstein/Arsenault/Das [4] showed that specific tap output values on a surface acoustic wave (SAW) device represented a signal's spectral components. Thus, a SAW device can be used to perform real-time Fourier transformations and inversions. The paper also mentioned that other transforms could be implemented using this device. Using the SAW device allows the use of ideal filters, a process known as *transform domain* (TD) processing. From this discovery, many filters were designed in the transform domain to remove interference. For most research, these new filters were implemented on a DSSS communication system. The traditional DSSS continues to serve as a baseline for comparing research results and will be used as such a comparison throughout this document.

In 1982, Milstein/Das/Gevargiz [5] compared the performance of a traditional DSSS system to a time-domain (TD) filtered DSSS system. Their results showed the traditional DSSS system required more processing gain to achieve the same bit error performance as the TD filtered DSSS, given equivalent bit energy. They concluded that a traditional DSSS system needs about a 10dB increase in processing gain to perform as well as a TDCS.

Although transform domain filtering techniques effectively remove interference, they also removed some desired signal energy. If a signal can be designed to avoid spectral regions where interference exists, then TD filtering can be employed without decreasing the desired signal energy level.

In 1989, German [3] analyzed a system where TD processing was performed in both the transmitter and receiver. The Andren/Harris corporation [1] subsequently received a patent in 1991 for a LPI communication system similar to the one proposed by German. These systems use transform domain processing to spectrally shape the waveform in the transform domain and avoid areas containing interference.

In 1996, Radcliffe [7] developed MATLAB® code to model and simulate the system defined by the Andren/Harris Corp and German. His results showed the improvement of a TDCS over a traditional DSSS for all the interference cases previously described.

In 1999, Swackhammer [12] extended Radcliffe's work and researched the use of TDCS techniques in a multiple access environment. His results showed that the TDCS is capable of supporting multiple users under specific parameter conditions.

In 2000, Roberts [9] modified Radcliffe's work to investigate TDCS synchronization issues – all previous work assumed perfect synchronization. Roberts focused on coarse synchronization (acquisition) and showed that the TDCS is capable of coarse synchronization with input SNRs as low as -23.0 dB.

1.2 Problem Statement

Previous work by Radcliffe, Swackhammer, and Roberts used the same TDCS architecture and spectral estimation technique – a 10th-order autoregressive (AR) filter. The filter provides a smooth (less response due to noise) spectral estimate, but by smoothing, it spectrally spreads the energy across the frequency scale. Subsequently, the spectral notching process captures a spectral region that actually extends beyond the interference region(s). This inefficiency may lead to a situation where the system cannot effectively communicate. The AR filter implementation also fails to correctly estimate the spectral content under swept-tone interference conditions – the lack of stationarity affects AR filter performance. Therefore, another spectral estimation technique needs to be considered; this research investigates the performance of a proposed wavelet-based spectral estimation technique with application to a TDCS.

1.3 Assumptions

This research is based on the following assumptions:

1. The communication channel can be represented as an AWGN source.

2. No multi-path interference exists. Methods exist to handle multi-path (e.g., RAKE receivers) and are assumed capable of fully mitigating multi-path effects [6].

3. Transmitter/receiver synchronization can be fully achieved. Previous work indicates a TDCS is capable of achieving synchronization [9].

4. Doppler effects are negligible, i.e., the transmitter and receiver are stationary with respect to each other.

5. The particular spectral location of the communication signals is not a factor in study. Results are generally extendable to any spectral region.

6. The TDCS is operating in a single transmitter-receiver scenario.

7. The receiver and transmitter are able to 'see' the same electromagnetic environment.

1.4 Scope

This research is limited to modeling, simulation, and analysis of spectral estimation algorithms using wavelet-based transformations and their incorporation into a TDCS architecture. This research closely parallels previous developmental TDCS research, including MATLAB® model modifications to permit evaluation of wavelet-based spectral estimation – referred to as a wavelet domain communication system (WDCS). The proposed WDCS bit error performance is evaluated under different interference scenarios and compared with the traditional DSSS system and the developmental TDCS for binary signal modulation.

1.5 Approach

Previous developmental TDCS work was used as a starting point for defining and evaluating a newly proposed WDCS. Given the previous TDCS architecture/structure [7], the spectral estimation process was targeted as an area of potential improvement – the previous TDCS failed to effectively estimate the swept-tone interference scenario. A wavelet transform is considered, providing a form of time-frequency analysis. The WDCS system is modeled using MATLAB® and simulation results compared with predicted (theoretical) results for several different interference scenarios. The bit error performance results are compared to a traditional *interference suppressing* DSSS and the developmental *interference avoiding* TDCS of previous research.

1.6 Materials and Equipment

Simulations were developed in MATLAB® Version 5.3, from The Mathworks Inc., Natick, MA. The simulations were run on Sun Ultra® workstations in computer labs at the Air Force Institute of Technology (AFIT).

1.7 Thesis Organization

Chapter 2 presents background information on the developmental transform domain communication system (TDCS) and the AR spectral estimation algorithm. Information presented on the TDCS includes overall system architecture and specific design parameters and their effects on overall system performance. Chapter 3 provides an overview of computer simulations used in the research, as well as insight on common signal representations used for computer simulation of communication systems. Chapter 4 presents research results and analysis based on descriptions provided in Chapter 3. Finally, Chapter 5 presents conclusion and

proposes recommendations for future research. Appendix A contains a complete acronym list and Appendix B contains a copy of the MATLAB® code developed under this research.

CHAPTER 2

BACKGROUND

2.1 Introduction

This chapter presents background material on a developmental transform domain communication system (TDCS) and the auto-regressive (AR) spectral estimation algorithm is uses. Section 2.2 describes the basic TDCS transmitter and receiver design, including operational details and results from previous TDCS research.

2.2 Transform Domain Communication System (TDCS)

The following sections provide an overview of the developmental TDCS transmitter and receiver design as used in previous research. The only transform implemented in the previous AFIT theses with the TDCS has been the Fourier transform.

2.2.1 Developmental TDCS Transmitter Design/Architecture

The developmental TDCS transmitter block diagram is shown in Figure 1. Using the Fourier transform, the transmitter estimates the spectrum and determines a spectral notching threshold based on estimate characteristics. Spectral regions exceeding the threshold are retained (spectral coefficients assigned a value of one) and spectral components below the threshold are "notched out" (spectral coefficient weights set equal to zero). A pseudo-random (PR) phase weighting is then applied to each element creating the "notched" vector of complex elements having uniform magnitude and PR phase. The elements are then scaled and an inverse Fourier transformed to create the time-domain waveform, called a *basis function*. The stored BF waveform is subsequently data modulated and transmitted.

Estimate
Spectrum

Spectrum
Magnitude

$A'(\omega)$

TX $s(t)$

$B_b(\omega)$ Scale $B(\omega)$ FFT^{-1} $b(t)$ Memory   Modulate
                  C

$e^{j\Theta(\omega)}$

Random
Phase

$d(t)$
Data
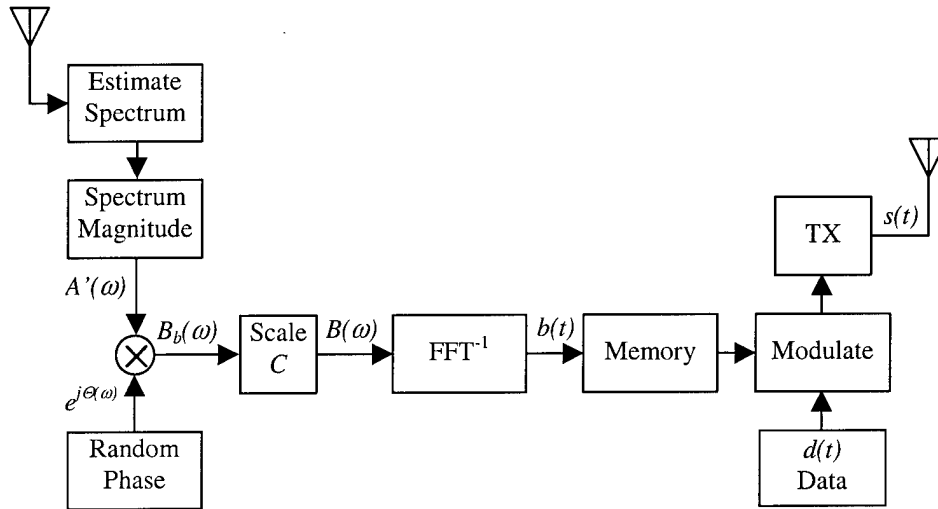
Figure 1. TDCS Transmitter Block Diagram [7]

2.2.1.1 Spectral Estimation

The basic concept of an interference avoiding TDCS is to avoid transmitting energy in spectral regions containing significant levels of interference. Therefore, the ability to accurately locate interference is vital to overall system performance. If the interference location process performs poorly, the induced errors propagate through the entire system and effectiveness is reduced.

One obvious solution to estimating the spectrum is to use the Fourier transform (FT), given the resultant coefficients represent signal energy distribution. The FT (and variants thereof) is one of the most widely used transformations and several optimized computer algorithm designs exist to quickly (efficiently) calculate the FT coefficients, e.g., the Fast Fourier Transform (FFT). The FFT is based on the Discrete Fourier Transform (DFT) and is computationally efficient if the number of signal samples is a power of two.

A *periodogram* provides an estimate of signal Power Spectral Density (PSD), i.e., the distribution of power as a function of frequency. The PSD of signal x(t), $S_x(\omega)$, is the FT of its autocorrelation, $R_x(\tau)$, [9], [7], [11], [10] as shown in (1).

$$S_x(\omega) = \Im\{R_x(\tau)\} \tag{1}$$

Equation (1) can be rewritten as shown in (2) [11], where $X_T(\omega)$ is the FT of x(t) over (-T/2,T/2).

$$S_x(\omega) = \lim_{T \to \infty}\left(E\left\{\frac{|X_T(\omega)|^2}{T}\right\}\right) \tag{2}$$

The limit as *T* approaches infinity is not a realistic case due to the finite amount of data, so the discrete version $(X_N(\omega), S_N(\omega))$ is implemented [11] and (2) can be rewritten as (3).

$$S_N(\omega) = \frac{|X_N(\omega)|^2}{N} \tag{3}$$

Figure 2 is the periodogram of a partial-band, Additive White Gaussian Noise (AWGN), interference source.
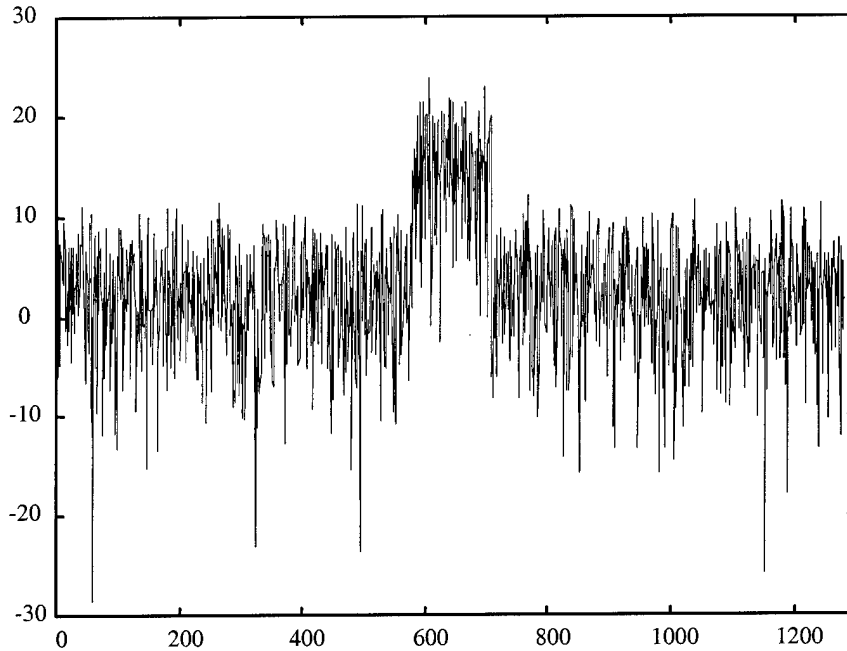
Figure 2. Periodogram of Partial-Band, AWGN Interference.

The periodogram is a noisy estimate. This leads to a desire for smoother spectral estimates, which in turn led to the use of an Autoregressive (AR) filter. The developmental TDCS uses a 10th-order AR filter for spectral estimation [7]. This filter provides spectral estimates, under both partial-band and multiple-tone interference scenarios, that are smooth enough to obtain consistent/reliable simulation results. Figure 3 is the periodogram representation for a scenario containing two single-tone interferers in AWGN. Figure 4 is the corresponding AR estimate, which is less noisy.
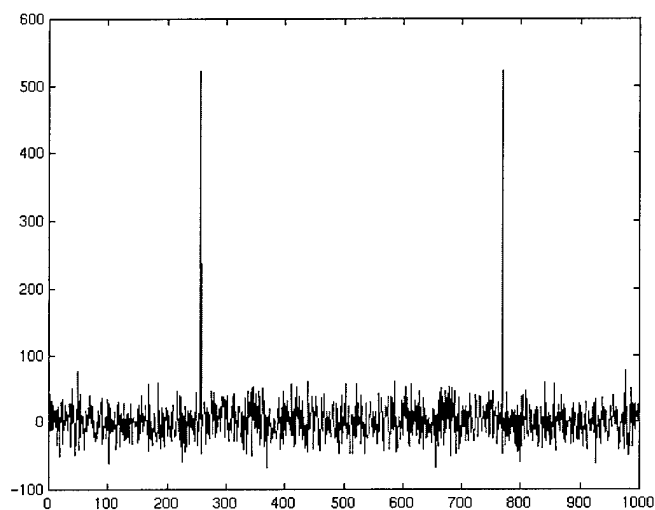
Figure 3. Two Single-Tone Interferers in AWGN.
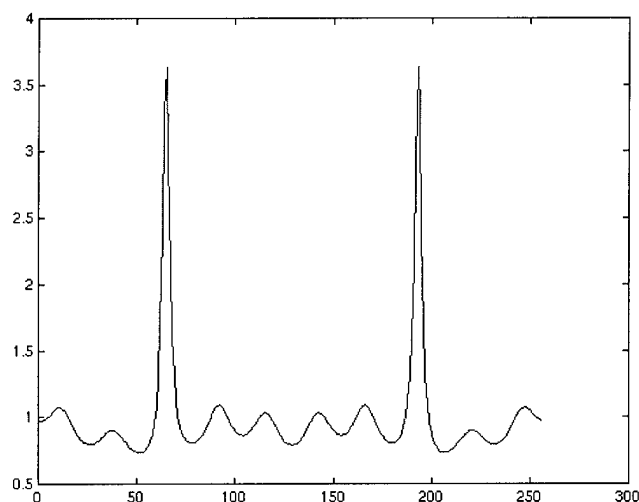
Figure 4. AR Estimate for Two Single-Tone Interferers of Figure 3.

2.2.1.2 Thresholding and Spectral Notching

After spectral estimation, the TDCS transmitter identifies where significant interference energy exists and establishes a threshold value to use for notching. For the developmental TDCS, a threshold value equaling 40% of the peak AR estimate is used [7] – three different percentages (33, 40, and 50) were evaluated and 40% was chosen based on overall acceptable/comparable performance versus the time required for computations. Spectral regions

exceeding the threshold are retained (spectral coefficients assigned a value of one) and spectral components below the threshold are "notched out" (spectral coefficient weights set equal to zero). This particular thresholding and notching process (as used in the developmental TDCS under consideration) yields the unit-amplitude rectangular waveform (vector) identified as A'(ω) in Figure 1. Although rectangular shaping has been shown to be effective, it has not been proven optimal [7], [9], [12]. Applying this process to the AR estimate of Figure (4), results in the rectangular notched waveform of Figure 5.
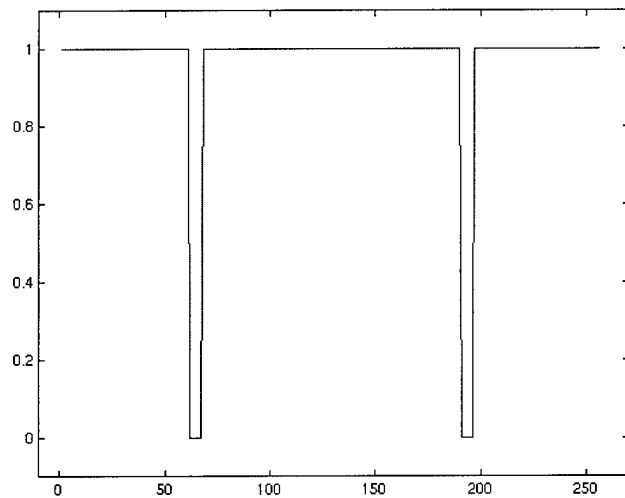
Figure 5. Notched Rectangular Waveform, A' (ω), for AR Estimate of Figure 4.

2.2.1.3 Phase Mapping Process

The thresholding/notching process serves to characterize the magnitude of the spectral estimate under consideration. Since the Fourier transform (complex) is employed, the phase characteristics of the estimate can be modified before taking the inverse transform – termed *phase mapping*. The developmental TDCS uses a phase mapping process based on a pseudorandom (PR) code, similar to those used in spread spectrum systems, to assign a specific phase weight to each element of the notched rectangular waveform. The particular phase

14

weights used for this research are derived from a maximal-length, linear feedback shift register (LFSR) configuration and phase mapping process as shown in Figure 6.
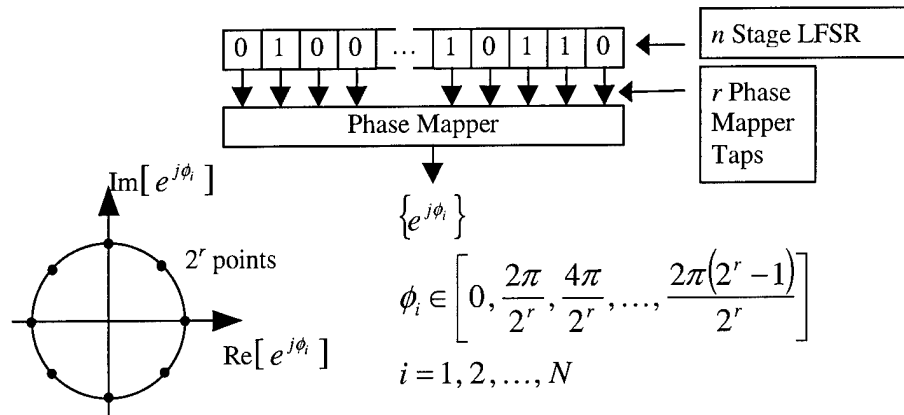
Figure 6. Developmental TDCS Pseudo-Random Phase Mapping Process [12].

Properly configured, an n-stage LFSR configuration produces a periodic PR code of length 2^n-1 (maximal length conditions). The phase mapper uses r LFSR taps ($r \leq n$) and successively assigns one of 2^r possible phase values to each element of the notched magnitude vector – the LFSR contents are shifted (clocked) s times for each phase value produced. The magnitude and phase vectors are multiplied together, element-by-element, and scaled by C (a constant) in a process called *phase coding* (4) and produce the vector B(ω) in Figure 1.

$$B(\omega) = C A'(\omega) e^{j\Theta(\omega)} \tag{4}$$

Swackhammer researched the relationship between various phase mapping parameters and identified an appropriate set for TDCS implementation [12].

2.2.1.4 Basis Function Generation and Modulation

The output of the phase mapping process is scaled to obtain a desired signal energy level. The scaled waveform is then inverse transformed to form the time-domain *basis function* (BF), b(t), used as a basic waveform for data modulation. The BF is stored in memory and subsequently modulated by the data. A representative TDCS BF is shown in Figure 7.

15
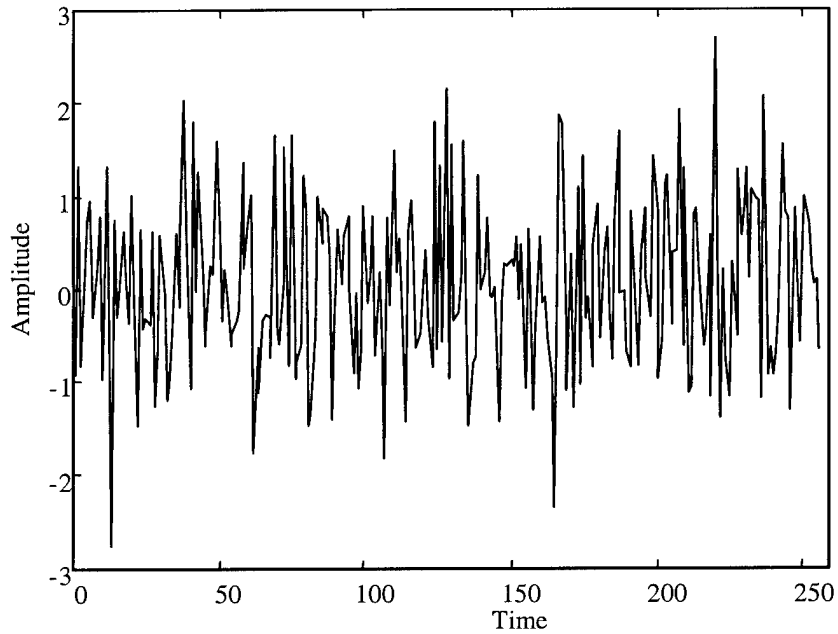
Figure 7. Representative TDCS Basis Function.

Two forms of modulation were considered for this research, antipodal and orthogonal. Antipodal modulation is a form of binary modulation that uses the BF as one symbol, $s_1(t)$, and the negated BF as the second symbol, $s_2(t)$.

$$
\begin{aligned}
s_1(t) &= BF \\
s_2(t) &= -s_1(t)
\end{aligned}
$$

(5)

Bit error probability, P_b, for antipodal signaling over an AWGN channel is given by (6) [10].

$$P_b = Q\left(\sqrt{\frac{2E_b}{N_0}}\right)$$

(6)

where E_b is the average energy per bit and N_0 is the noise power density. The Q-function is the Complementary Error Function, defined in (7) [10].

$$Q(x) = \int_x^\infty \frac{1}{\sqrt{2\pi}} e^{-\frac{z^2}{2}} dz$$

(7)

16

In orthogonal signaling, the symbols are separated by $90°$, as opposed to $180°$ with antipodal signaling. Smaller communication symbol separation produces larger bit error probabilities while allowing for M-ary signaling.

Two signals are deemed orthogonal if their cross-correlation is zero for given a time interval [0,T]. This is shown in (8) where k is a non-zero number.

$$\int_0^T s_i(t)s_j^*(t)dt = \begin{cases} k & i = j \\ 0 & i \neq j \end{cases} \tag{8}$$

For orthogonal signaling, the bit error probability is given by (9) [10].

$$P_b = Q\left(\sqrt{\frac{E_b}{N_0}}\right) \tag{9}$$

A form of cyclic shift keying (CSK) was the form of orthogonal signaling considered for this research. CSK uses circular shifts of the BF to represent different communication symbols. The process of creating symbols for M-ary CSK modulation is shown in (10). The M-ary CSK probability of symbol error is given by (11) where E_s is the average energy per symbol and each symbol represents $\log_2(M)$ bits. For the binary signaling case, each symbol represents one bit and the probability of symbol error equals the probability of bit error.

$$s_1(t) = b(t) \equiv Basis\ Function\ (BF)$$
$$s_M(t) = b\left(\left(t - \frac{T}{M}\right)\right)_T \tag{10}$$

$$P_E(M) \leq (M-1)Q\left(\sqrt{\frac{E_s}{N_o}}\right) \tag{11}$$

Sample plots of antipodal and BCSK modulated symbols are shown in Figure 8. These plots are based on the sample BF in Figure 7.
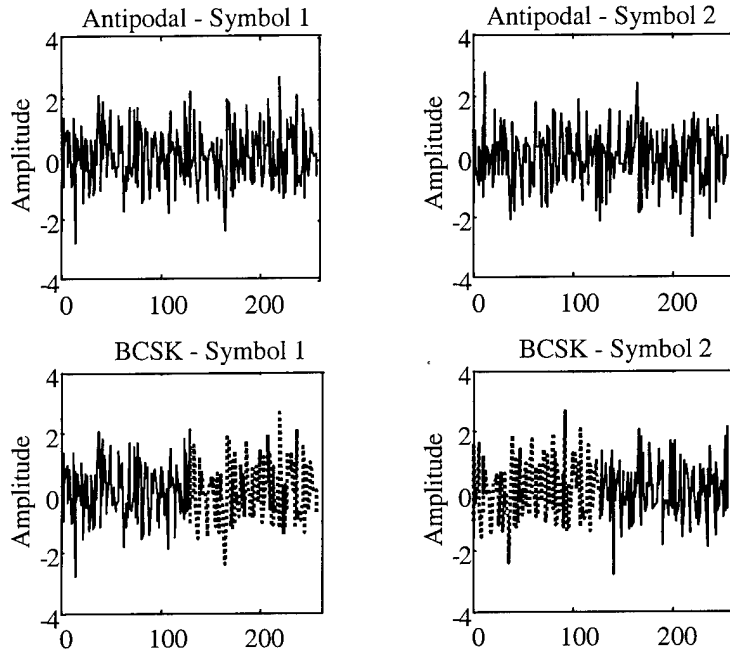
Figure 8. Antipodal (Top) and BCSK (Bottom) Modulation Symbols for b(t) of Figure 7.

2.2.1.5 Basis Function Timing Generation

Synchronization and timing are important issues in characterizing developmental TDCS performance. Both transmitter and receiver must perform BF generation operations at the same time (the assumption being they simultaneously 'see' the same electromagnetic environment and generate identical BFs) – this is essential for reliable symbol demodulation/estimation. The overall BF generation process includes transforming the sampled environment, establishing/setting a threshold limit, notching spectral regions exceeding the threshold, phase mapping and coding, scaling, inverse transforming to the time domain, and storing/modulating the resultant BF – operations which must occur autonomously at the transmitter and receiver locations. The longer the system operates without resampling the environment, the more opportunity there is for spectral change and bit error rate increases. On the other hand, shorter

resampling intervals help to minimize the sensitivity to environmental change. Although important (perhaps critical), these timing related issues are operational in nature and beyond the scope of this research. The assumption maintained throughout this research, as in previous research, is that the transmitter and receiver are capable of generating identical basis functions.

2.2.2 Previous Research Results

Previous research on the developmental TDCS used probability of bit error as the key metric for performance comparisons. The developmental TDCS was modeled and simulation results obtained for various interference scenarios, including partial-band, single-tone, multiple-tone, and swept-tone. The partial-band scenarios included interference energy covering 10% to 80% of the system bandwidth. The multiple-tone scenarios consisted of seven different tones, evenly spaced across the spectrum, with the center tone located at the center of the system's bandwidth. Developmental TDCS performance results are presented (as needed) in Chapter 3 for comparison with results of this research – in all cases, the TDCS test scenarios and test conditions were duplicated exactly to ensure valid comparisons could be made. Of particular importance, the developmental TDCS could not effectively estimate swept-tone interference using the AR model and resorted to using periodogram estimation to obtain simulation results. Therefore, the TDCS performance against swept-tone interference was shown to be sub-optimal by comparison with the other interference scenarios considered; one weakness specifically addressed by this research and the proposed WDCS.

2.3 Summary

This chapter presented information on previous research related to a developmental TDCS. A description of the TDCS model and associated simulation scenarios were introduced. The

inadequacy of the TDCS to correctly model the swept-tone interference is the motivation behind

this research.

CHAPTER 3

METHODOLOGY

3.1   Introduction

Section 3.2 describes the WDCS model as it is compared to the developmental TDCS model. Section 3.3 describes the visual interpretation of wavelet decomposition when used as spectral estimation. Section 3.4 describes the various thresholding techniques investigated. Section 3.5 describes the phase mapping and encoding process. Section 3.6 describes the models used to generate interference signals. Section 3.7 describes the basis function generation. Section 3.8 describes the metrics used for model verification and validation.

3.2   Wavelet Domain Communication System (WDCS) Model vs. TDCS

The basic TDCS model used for comparative analysis, shown in Figure 1, includes a Fourier-based spectral estimation block and Fourier-based inverse transform block. The proposed WDCS model is represented by an identical diagram with the exception that the spectral estimation block/process is implemented with a specific wavelet transform technique; by necessity, the generic inverse transform block producing the basis function becomes an inverse wavelet transform. In reality, the original computer modeling code was modified such that any transform technique could be inserted into the process model. The remaining components of the original TDCS block diagram are unchanged, allowing results to be directly comparable between the two systems under consideration.

21

3.3   Wavelet Domain Spectral Estimation

The wavelet transform produces information that can be represented graphically using two axes, a scale axis (related to frequency) and a time axis. Fundamentally, the wavelet transform is implemented using a series of iterations and recursive processing. The first transform iteration divides the samples into two bins; one for detail coefficients and the other for coarse coefficients. The detailed bin coefficients represent the effect of passing the original signal through a high pass filter. The coarse bin coefficients represent the effect of passing the signal through a low pass filter. The second transform iteration performs the same operation as the first iteration except that the transform is now applied to the coarse bin coefficients. This iterative processing continues a user-defined number of times. The final transformed data can be represented in one of two different ways, either in matrix form or as a vector. Visually, the data is better represented using the matrix form with each row representing a different scale resolution and each column representing a different time resolution, shown in Figure 9. Computationally, the data is better handled if it is in vector form, shown in Figure 10.
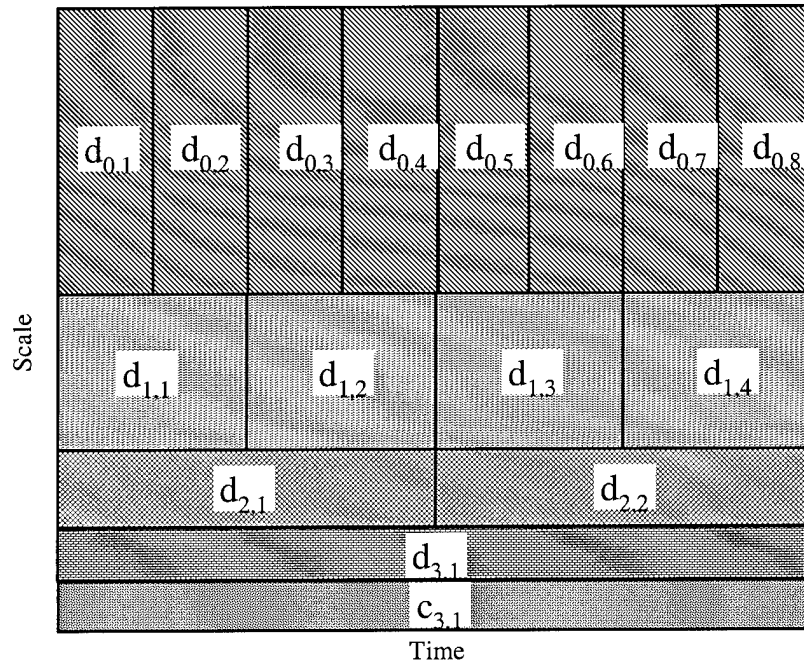
Figure 9. Matrix Representation of Wavelet Decomposition
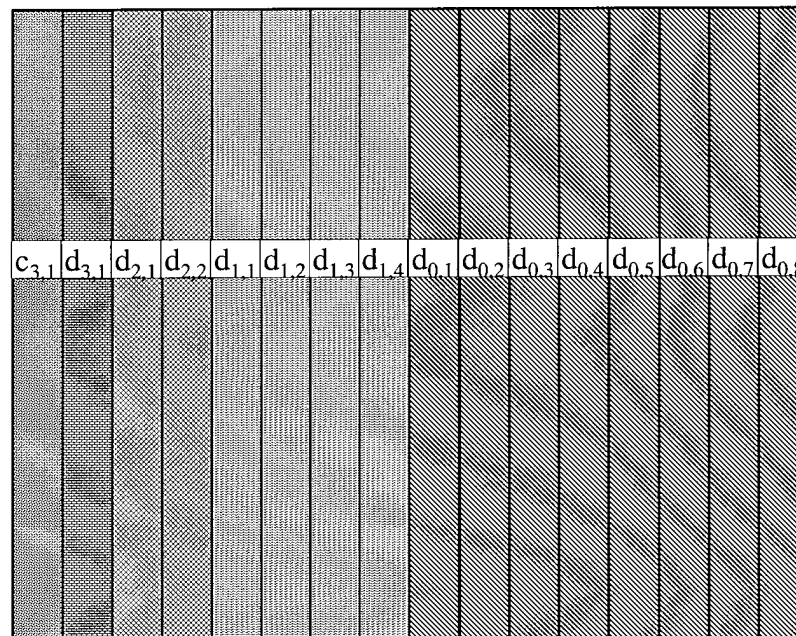
Figure 10. Vector Representation of Wavelet Decomposition

3.3.1 Mother Wavelet

It is the scaling and translation of the 'mother wavelet' that correlates with the sampled environment to produce the spectral estimation. The scaling and translation operation is shown in (12) where Z is the set of all integers. The variable 'j' represents the scaling and 'k' represents the translation [2].

$$\Psi_{j,k}(t) = 2^{\frac{j}{2}} \Psi(2^j t - k) \qquad j, k \in Z \qquad (12)$$

There are many different mother wavelets to use. It is desirable for the mother wavelet to have certain properties. If it can form an orthonormal basis, then Parseval's theorem applies and the energy of the signal in the time domain is equal to the energy of the coefficients in the wavelet domain. Another desirable property is compact support. If the wavelet is nonzero over a finite region, there will be fewer calculations to be made and time localization is possible [2]. For this research, a Daubechies 8 mother wavelet was used. It is both orthonormal and compactly supported. There is no claim that this choice is optimal; it is simply a well-known wavelet. The time domain representation of a Daubechies 8 is shown in Figure 11.
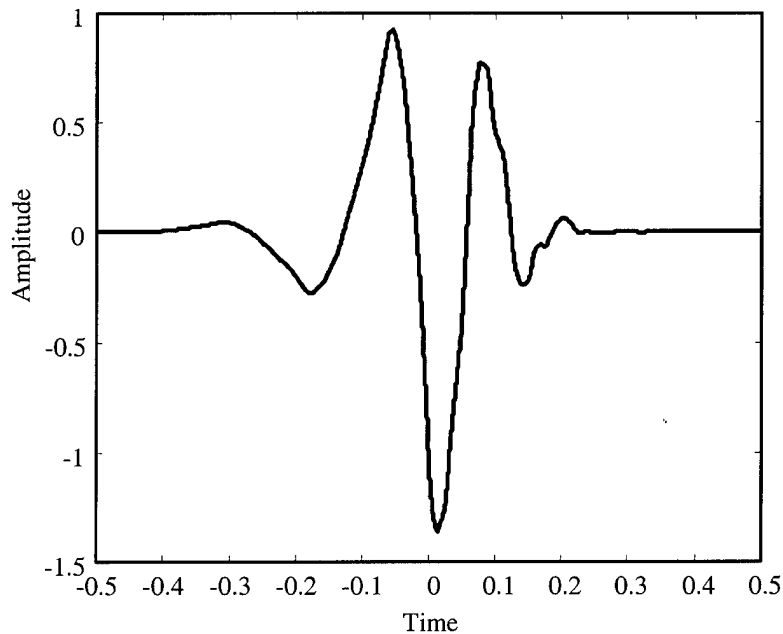
Figure 11. Time Domain Representation of a Daubechies 8 Wavelet.

3.4 Threshold Determination

Two different wavelet thresholding schemes were investigated; the first involved applying the threshold on a sample-by-sample basis and the second involved applying independent thresholds on a subband-by-subband basis. Although thresholding on a sample-by-sample basis within a wavelet subband is an option, the technique proved ineffective for some realistic operating conditions. Since samples within a wavelet subband represent different time shifts, applying a sample dependent threshold assumes the system is synchronized with the interference. This assumption is not valid in two specific scenarios, including the cases when 1) the interference is not present during the entire environmental sampling interval, and 2) swept-tone interference is present. In the first scenario, the interference is not present during the entire observation interval, yet the effects of removing it are evident throughout the entire transmission period. This leads to inaccurate estimation and results in poorer (higher) bit error performance. The second scenario involves the presence of swept-tone interference exhibiting a specific

25

(perhaps variable) sweep period. If the WDCS cannot synchronize to the sweep period, the swept-tone interference will represent different time shifts throughout both the observation and transmission periods; resulting in poorer bit error performance. Since these two scenarios are realistic, the sample-by-sample thresholding scheme was abandoned and not considered a viable alternative for this WDCS research.

The second thresholding scheme involves applying independent thresholds on a subband-by-subband basis, i.e., entire subbands are either nulled-out (coefficients set equal to '0') or retained (coefficients set equal 1). This process effectively mitigates the problem of requiring synchronization with the interference since time information is not used. However, there are potential problems with this scheme because of the different subband sample sizes. The number of wavelet subband samples starts at one-half the total number of samples ('highest' subband) and decreases progressively by a factor of two down to one ('lowest' subband). The amount of interference information contained within specific subbands, combined with the thresholding technique implemented, has a direct effect on overall WDCS performance. For example, a single-tone interferer can have energy in any one of the wavelet subbands. If this energy appears in the highest subband, and is significant enough to cause this subband to be nulled-out, then one-half of the original signal coefficients are nulled-out and not available for communication. However, if the interference energy occupies the next lowest subband, then only one-fourth of the samples are nulled-out and more coefficients remain for communication. Variation in interference location within the system's bandwidth and its effect on WDCS performance was beyond the scope of this research and not investigated - all interference scenarios were centered within the system's bandwidth.

The actual threshold value used in the subband-by-subband thresholding scheme was based on comparing the a-priori noise power (noise power before interference) and the individual subband powers with interference present. When individual subband power exceeds the noise power level, interference is declared 'present' and the entire subband is nulled-out. Conversely, if the noise power level is not exceeded, all subband samples are assigned a value of '1'. This thresholding process proved to be effective and provides acceptable WDCS performance – there is no claim of optimality and proving the same was beyond the scope of this research.

3.5   Phase Mapping / Encoding

Previous research on the developmental TDCS encoded the phase information using point-by-point multiplication of a pseudo-random phase sequence with the notched spectral magnitude vector of 1's and 0's. The pseudo-random phase was generated by the phase mapping process shown in Figure 6. In the TDCS case, this operation was relatively easy and conceptually satisfying since each 1 and 0 in the vector represent a specific spectral component in the frequency domain – a 0 element simply corresponds to eliminating one of the Fourier sinusoidal components that will comprise the basis function. Things were not as intuitively obvious with the proposed WDCS, given the notched vector of 1's and 0's represents different things depending upon the notch location(s) within the vector. For example, a coefficient in the highest subband bin represents a specific amount of time and scale. A coefficient in the next lower subband bin represents a larger amount of time at a different scale. Initially, it was unclear as how the PR phase sequence should be applied to produce desired results. As a starting point, the point-by-point multiplication technique of the developmental TDCS was used and its performance analyzed. As supported by results presented in Section 4.2, this process proved to be effective and resulted in the basis functions having uniform phase distribution.

3.6   Signal Model / Interference Generation

Five distinct interference scenarios were generated using MATLAB®. The code for each scenario is included in APPENDIX B – Interference Code. Each interference source was modeled as a complex waveform and all sources had the same total average power. The interference scenarios were specifically designed to match the interference models used to characterize the developmental TDCS performance – valid performance comparison was the goal.

3.6.1   Partial Band Interference

The two partial-band interferers were modeled in similar ways. They were created in the frequency domain using a rectangular pulse of 1's and 0's, centered at one-fourth the sampling frequency (one-half the Nyquist frequency), and having a spectral width equivalent to the desired percentage of system bandwidth containing interference. For each simulation, a new random vector point multiplied the rectangular pulse to induce random phase and guarantee different interference realizations were used. The total interference power was controlled by adjusting the amplitude of the rectangular pulse. The time domain representation of the interference was simply generated by taking the inverse Fourier transform.

3.6.2   Single-Tone and Multiple-Tone Interference

The single-tone and multiple-tone interference were modeled using complex sinusoids. The single-tone interference frequency was set equal to one-half the Nyquist frequency. The multiple-tone interference consisted of seven equally spaced tones, with the center tone positioned at one-half the Nyquist frequency. A random starting phase was included to ensure a different realization occurred each time simulations were run. The total average power of the

single-tone interference was controlled by adjusting the sinusoid amplitude. In the multiple-tone case, the total average power was controlled by applying an amplitude weight to each tone equaling one-seventh the amplitude required for the single-tone.

3.6.3 Swept-Tone Interference

Two conditions were imposed on the swept-tone interference. First, the swept-tone interference remained within the system's bandwidth during the sweep interval. Second, each frequency sweep occurred during the observation/spectral estimation interval. These conditions ensured the spectral estimation algorithm had maximum opportunity to effectively estimate the interference. These two conditions are fundamentally related to (or impact) two system parameters, namely, observation time and sampling frequency. The swept-tone interference bandwidth was set equal to 60% of the system bandwidth and used a sweep rate equal to five symbol intervals. Therefore, in the time it takes to transmit five symbols, the interference has swept through its entire range of frequencies; after every five symbols are transmitted, the swept-tone interference resets to its lowest frequency and starts a new sweeping cycle.

3.7 Basis Function Generation

The WDCS basis function is generated using the same process as the developmental TDCS described in 2.2.1.4. The only difference is that the notched rectangular vector of 1's and 0's, which has been weighted by the random phase information, is inverse transformed using a wavelet transform versus the Fourier transform of the developmental TDCS. The resultant time-domain waveform is called the *basis function* and is subsequently stored and data modulated prior to transmission.

3.8 WDCS Model Verification and Validation

Each simulation process consists of 1) creating the desired interference, 2) adding AWGN, 3) sampling/estimating the environment, 4) thresholding the estimate, 5) notching/phase coding, 6) creating a BF, 7) transmitting 100 bits of data, 8) adding AWGN, 9) demodulating/estimating 100 bits, 10) calculating bit error rates, and 11) repeating the process until convergence criteria is satisfied. The convergence criteria chosen was 500 errors. This number was chosen because it produced smooth results without long processing time. There is no optimality implied. The primary metric used for system evaluation and performance comparison is the probability of bit error. The *communication performance* (non-interference scenarios) of the proposed WDCS is characterized using simulation results obtained for E_b/N_o values ranging between 0.0 dB and 8.0 dB. The *interference avoidance capability* of the proposed WDCS is evaluated using simulation results with E_b/N_o equal to 4.0 dB at *I/E* (interference energy-to-signal energy ratio) values ranging between 0.0 dB to 16.0 dB. In both cases, the performance of the proposed WDCS is compared to a traditional DSSS and a developmental, Fourier-based TDCS.

3.9 Summary

This chapter highlighted the similarities and differences between the proposed WDCS and a developmental TDCS. A description of the wavelet transformation process and its use in spectral estimation is also presented. Different thresholding techniques that were considered under the research are discussed, including how the random phase values are applied in the proposed system model. Attention is given to how the different interference sources are generated and how each is applied in specific simulation scenarios.

CHAPTER 4

SIMULATION RESULTS AND ANALYSIS

4.1   Introduction

This chapter reports results of the simulations discussed in Chapter 3. Section 4.2

describes basis function orthogonality, a desirable characteristic when optimal signal estimation

is required. Section 4.3 shows how the specific interferers used for this research 'appear' in the

wavelet domain following transformation. Section 4.4 provides simulation and analysis results

for each of the scenarios considered. Section 4.5 describes how WDCS performance compares

with other interference suppressing/avoiding systems.

4.2   Basis Function Orthogonality

The ability to use the CCSK modulation scheme requires the basis function to have

orthogonality. For this research, orthogonality was achieved using a phase coding process that

point multiplies a pseudo-random phase vector with a vector representing the wavelet transform

magnitude. After the inverse wavelet transform, the resulting basis function waveform shares

properties of AWGN —uniform phase distribution and orthogonal to cyclic shifts of itself.
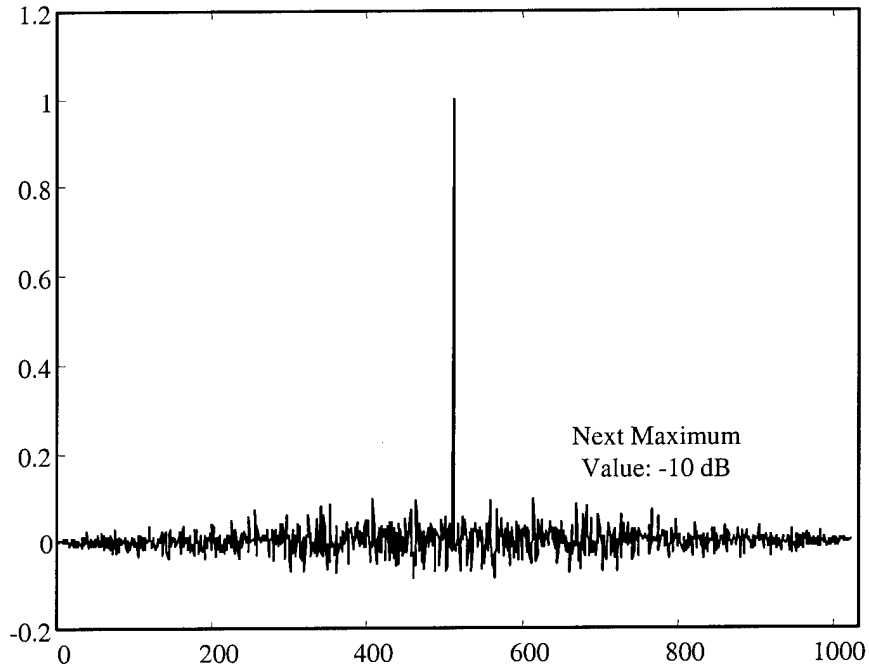
Figure 12. WDCS Basis Function Autocorrelation – Exhibits AWGN Characteristics.
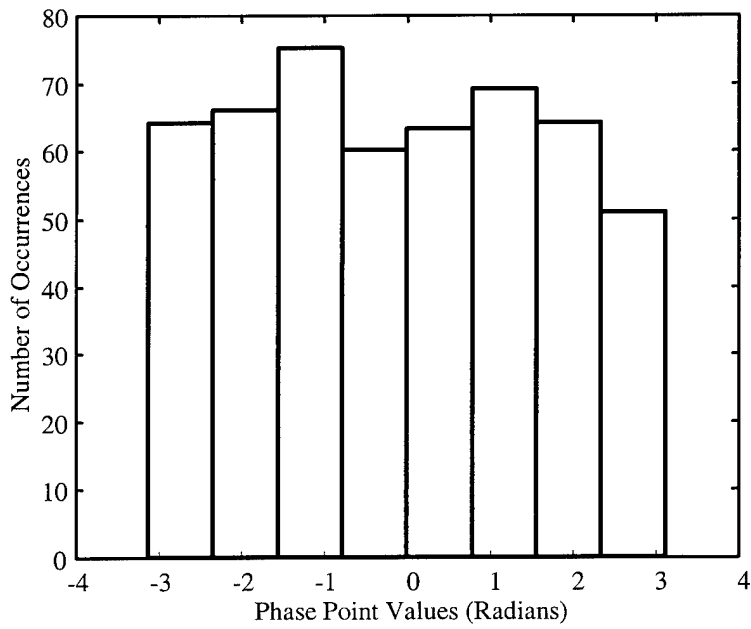
Figure 13. WDCS Basis Function Phase Histogram.

4.3 Wavelet Domain Representation of Various Interference Sources

Before modeling the proposed WDCS and evaluating its performance, it is instructive to consider what various interference sources 'look' like in the wavelet domain. Figure 14 through Figure 18 are the wavelet domain representation of various interference sources used in this research. Each figure contains two subplots with the top plot derived using interference only and the bottom plot derived from an interference source embedded in AWGN.
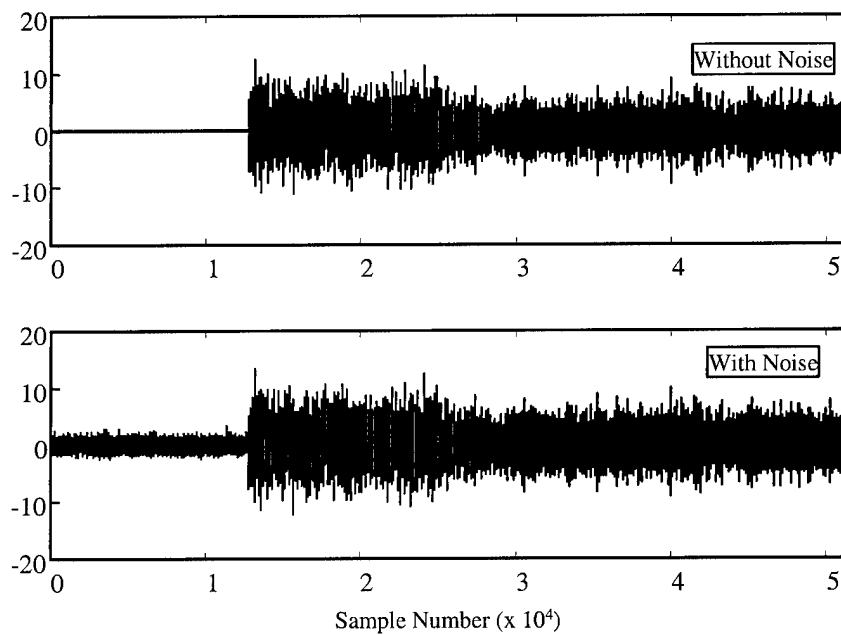
Figure 14. Wavelet Domain Transform: 10% Partial-Band Interference, Without AWGN (Top) and With AWGN (Bottom) for E_b/N_o = 4.0 dB and I/E = 10.0 dB.
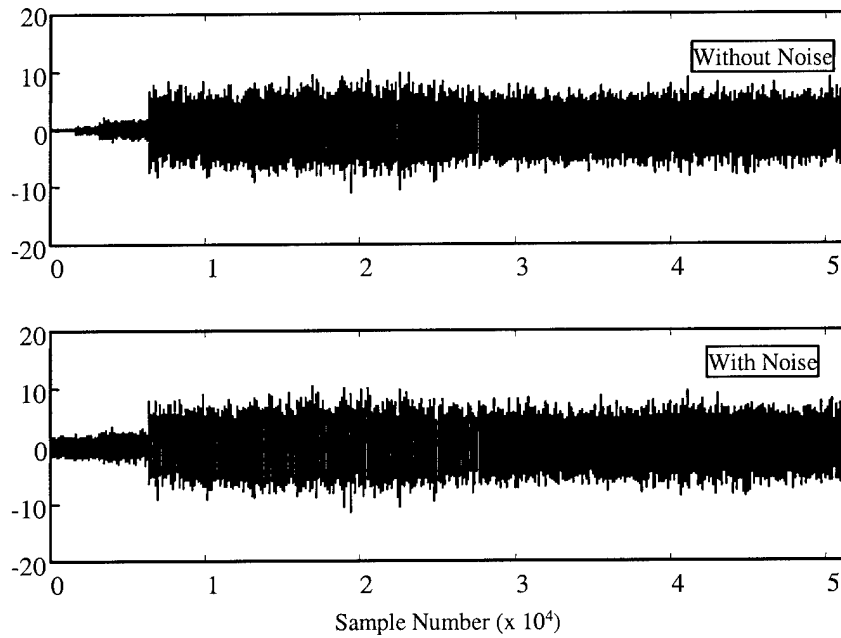
Figure 15. Wavelet Domain Transform: 70% Partial Band Interference, Without AWGN (Top) and With AWGN (Bottom) for E_b/N_o = 4.0 dB and I/E = 10.0 dB.
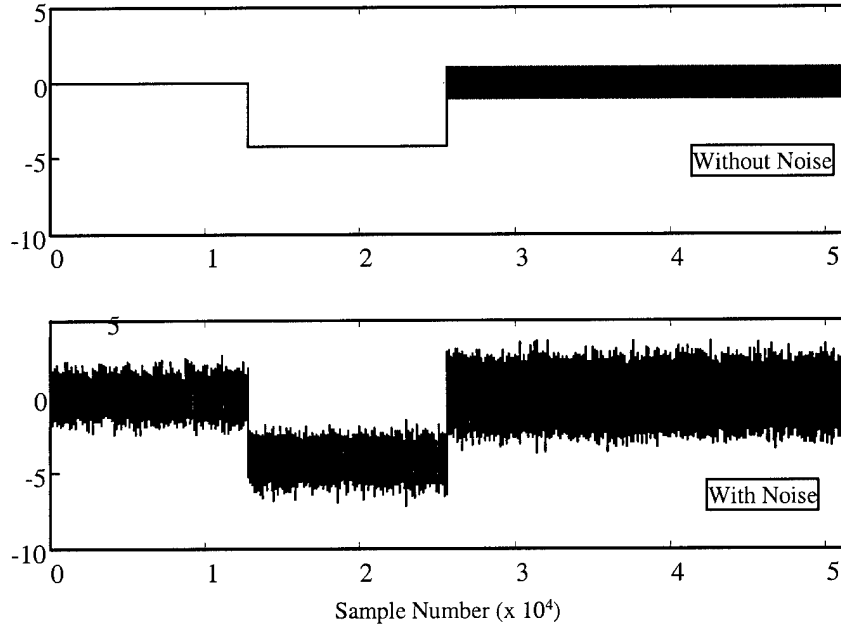
Figure 16. Wavelet Domain Transform: Single-Tone Interference, Without AWGN (Top) and With AWGN (Bottom) for E_b/N_o = 4.0 dB and I/E = 10.0 dB.
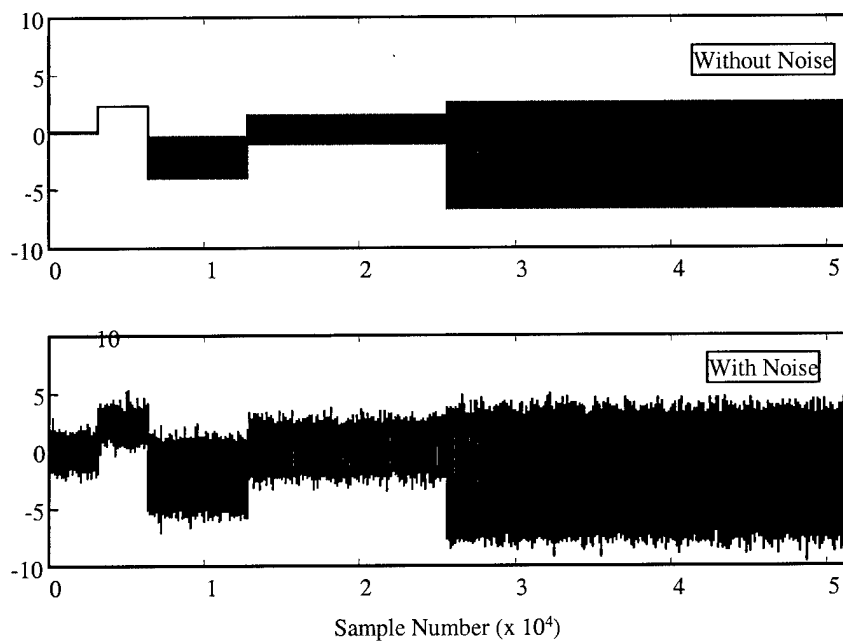
Figure 17. Wavelet Domain Transform: Multiple-Tone Interference, Without AWGN (Top) and With AWGN (Bottom) for E_b/N_o = 4.0 dB and I/E = 10.0 dB.
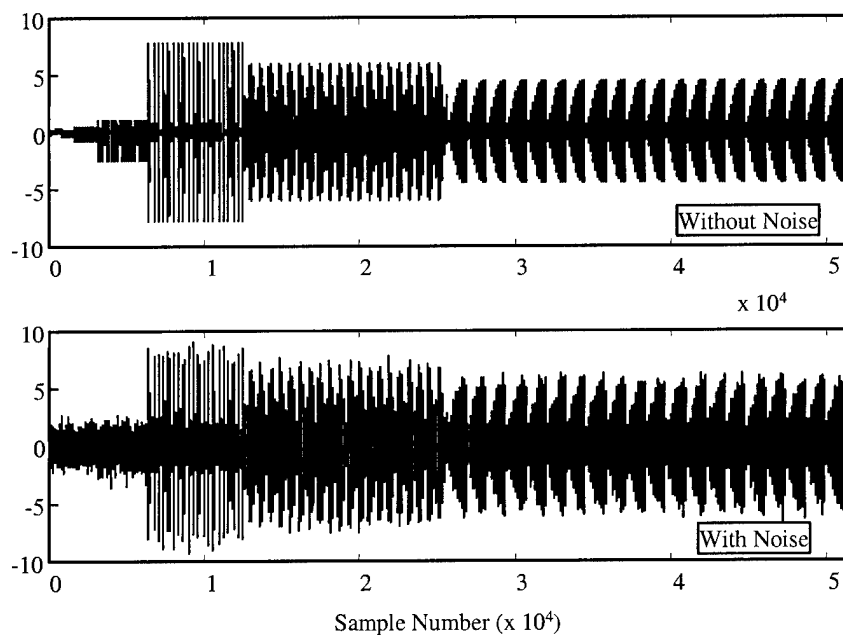
Figure 18. Wavelet Domain Transform: Swept-Tone Interference, Without AWGN (Top) and With AWGN (Bottom) for E_b/N_o = 4.0 dB and I/E = 10.0 dB.

4.4 Model Verification and Validation

4.4.1 Scenarios for AWGN Channel – No Interference Present

Simulations were run for all models in the absence of interference to ensure proper operation. Each simulation observed the environment for a length of time equaling 100 bits and then modulated/demodulated the bits while counting the errors. The simulations were terminated when the total number of bit errors, n, exceeded 500 - this number was chosen empirically and was sufficient to produce relatively smooth bit error curves. The observed bit error performance for antipodal modulation was calculated using (13)

$$P_b = \frac{n}{N} \tag{13}$$

where N is the total number of transmitted bits.

4.4.1.1 Antipodal Signaling

The theoretical bit error performance for antipodal modulation is given by [10],

$$P_b = Q\left(\sqrt{\frac{2E_b}{N_o}}\right) \tag{14}$$

As Figure 19 shows, the simulation results nearly match theoretical, antipodal signaling bit error performance – a mean absolute error of 8.9×10^{-4} and standard deviation of 1.1×10^{-3} over the range of indicated E_b/N_o values.
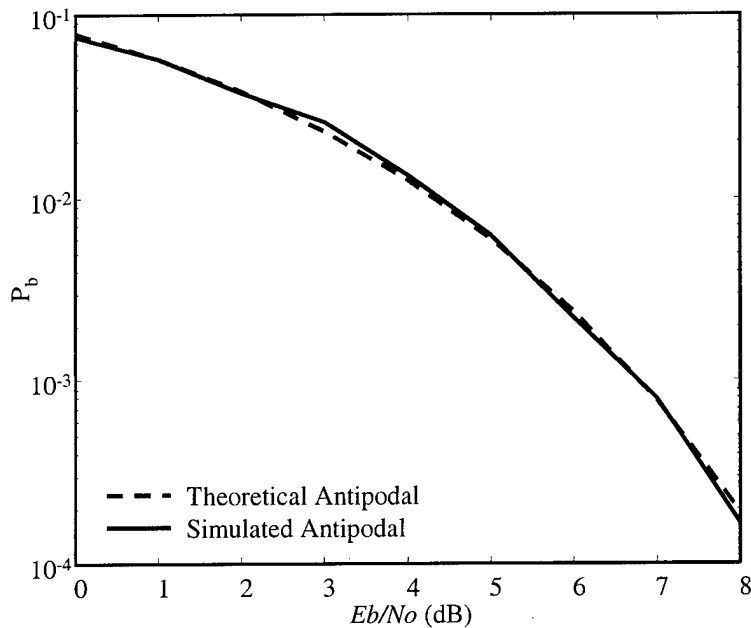
Figure 19. WDCS Antipodal Signaling Bit Error Performance Results.

4.4.1.2 Orthogonal Signaling – BCSK and BCASK Modulation

The theoretical bit error performance for orthogonal signaling is given by [10],

$$P_b = Q\left(\sqrt{\frac{E_b}{N_o}}\right) \tag{15}$$

Simulations were initially run using Binary Cyclic Shift Keying (BCSK), previously shown to be an effective form of orthogonal signaling for the TDCS [7]. For the WDCS under consideration here, simulation results indicate an obvious bias in bit error performance as illustrated in Figure 20. There is a mean absolute error value of 1.3×10^{-2} and standard deviation of 7.3×10^{-3} over the E_b/N_o values shown – the WDCS using BCSK modulation does not produce results consistent with orthogonal signaling. A newly proposed modulation scheme, termed *Binary Cyclic Antipodal Shift Keying* (BCASK), was considered next; this technique uses the same cyclic shift operation of BCSK but negates one-half the sample values prior to shifting. As indicated in Figure 20, the BCASK results closely match orthogonal signaling theoretical

37

performance – a mean absolute error value of 2.2×10^{-3} and standard deviation of 3.2×10^{-3} over the range of E_b/N_o values shown. Based on these results, the newly developed BCASK modulation technique was used exclusively for simulation of various interference scenarios.
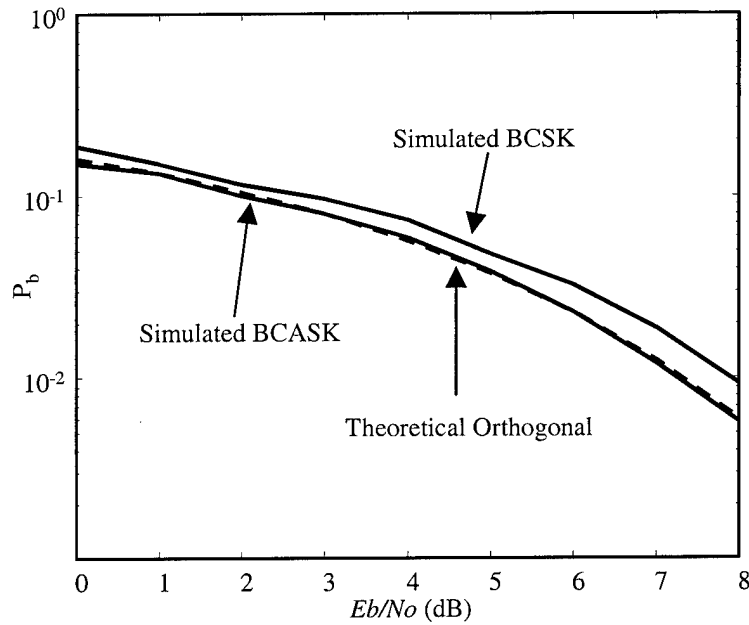
Figure 20. WDCS Orthogonal Signaling Bit Error Performance Results.

4.4.2 Scenarios for AWGN Channel, Interference Present, No Spectral Shaping

Simulation results were verified against theoretical performance for scenarios containing interference without employing spectral shaping, i.e., no wavelet subband thresholding/nulling is used. These results are important and establish a baseline for comparing various interference suppressing (DSSS) and interference avoiding (TDCS) systems. Here, theoretical performance is estimated by assuming constant interference power spectral density over the system bandwidth, effective adding to the system noise floor and impacting bit error performances per (14) for the antipodal signaling case and (15) for the orthogonal signaling case. **Figure 21** shows that for the antipodal signaling case, the partial band-interference (10% and 70%) results closely approximate the theoretical antipodal performance for all I/E values considered. However, the

tone interference results show some deviation, especially the single-tone interference scenario, which exhibits considerable deviation at lower I/E values.
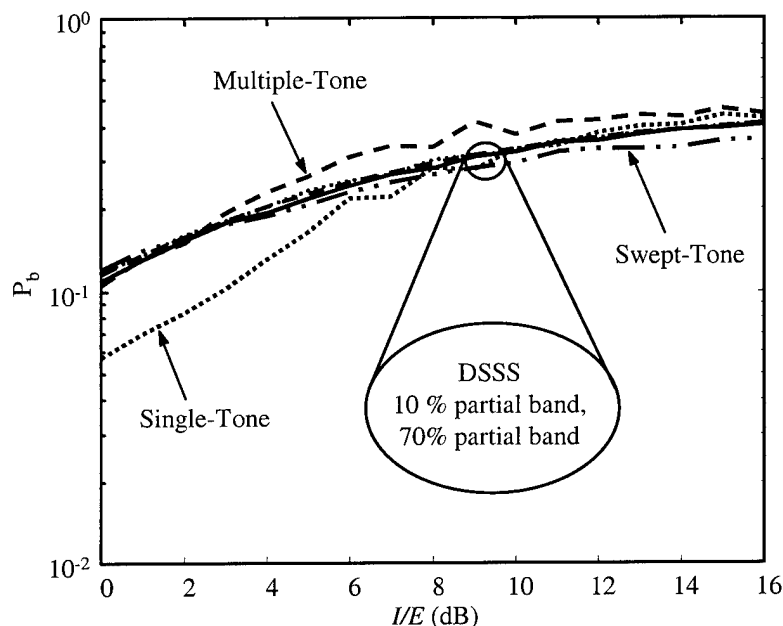
Figure 21. Antipodal Signaling Interference Results - No WDCS Spectral Shaping.

The orthogonal modulation (BCASK) interference results are shown in Figure 22. Consistent with the antipodal modulation case, the orthogonal partial-band interference results closely approximate the theoretical performance. However, in this case the swept-tone interference results also closely match. Both the single-tone and multiple-tone interference results deviate considerably.

The deviations noted in both the antipodal and orthogonal modulation cases are likely a result of the constant interference power spectral density assumption used for obtaining the theoretical results – an assumption clearly violated in the single-tone interference case. Therefore, the comparative analysis of simulation and theoretical results indicate the WDCS model is operating properly under the cases considered thus far.
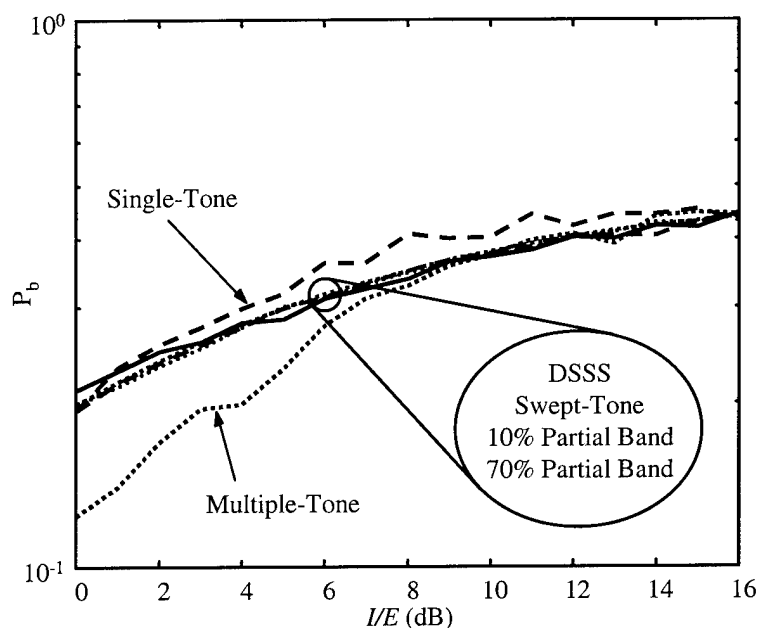
Figure 22. Orthogonal Signaling Interference Results – No WDCS Spectral shaping.

4.4.3 Scenarios for AWGN Channel, Interference Present, Spectral Shaping Included

After the model performance was verified with and without interference present, a series

of simulations were run that included WDCS spectral shaping – effectively a test of the

"interference avoidance" capability of the WDCS, i.e., a characterization of bit error

performance improvement relative to the data presented in Figure 21 and Figure 22. Partial-band

interference scenarios were first considered.

4.4.3.1 Partial-Band Interference Suppression – Spectral Shaping Employed

By comparison with Figure 21, Figure 23 results indicate the achievable bit error

improvement (interference avoidance capability) provided by the WDCS for partial-band

interference scenarios when using antipodal modulation and spectral shaping (subband nulling).

Likewise, by comparing Figure 22 and Figure 24 results, the achievable bit error improvement

provided by orthogonal modulation is evident. In both modulation cases, improvement degrades

as the I/E ratio increases but still outperforms the case when no spectral shaping is employed.

Figure 23. Partial-Band Interference: Antipodal Modulation with Spectral Shaping.
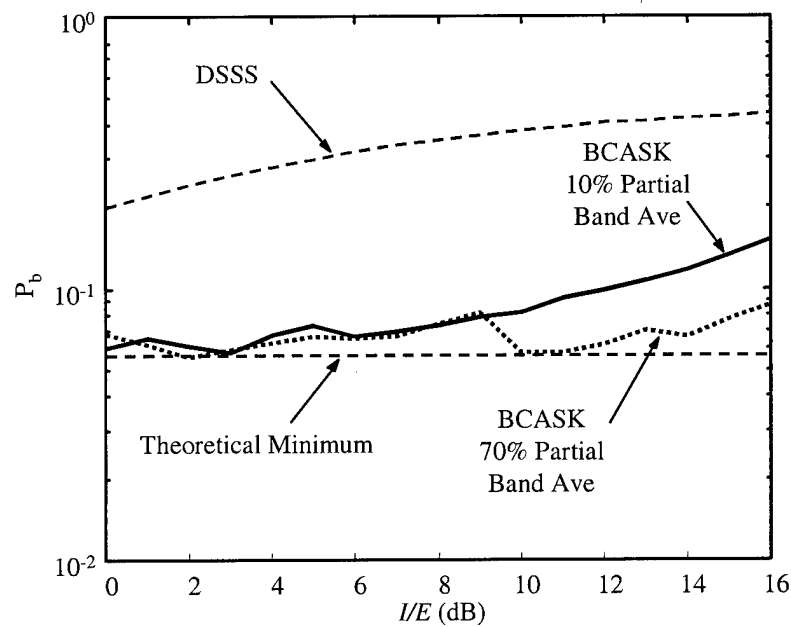
Figure 24. Partial-Band Interference: Orthogonal BCASK Modulation with Spectral Shaping.

41

4.4.3.2 Single-Tone and Multiple-Tone Interference – Spectral Shaping Employed

Simulations involving single-tone and multiple-tone interference were next considered. For scenarios containing both single-tone and multiple-tone interference, a WDCS using antipodal modulation with spectral shaping successfully suppresses the interference effects as illustrated in Figure 25; in all cases, the simulation results closely approximate the theoretical performance of an interference-free environment. As indicated in Figure 26, the WDCS orthogonal BCASK modulation technique effectively mitigates the single-tone interference. However, the WDCS BCASK technique appears far less effective in scenarios containing multiple-tone interference – although bit error performance is better than the case where no spectral shaping is employed.
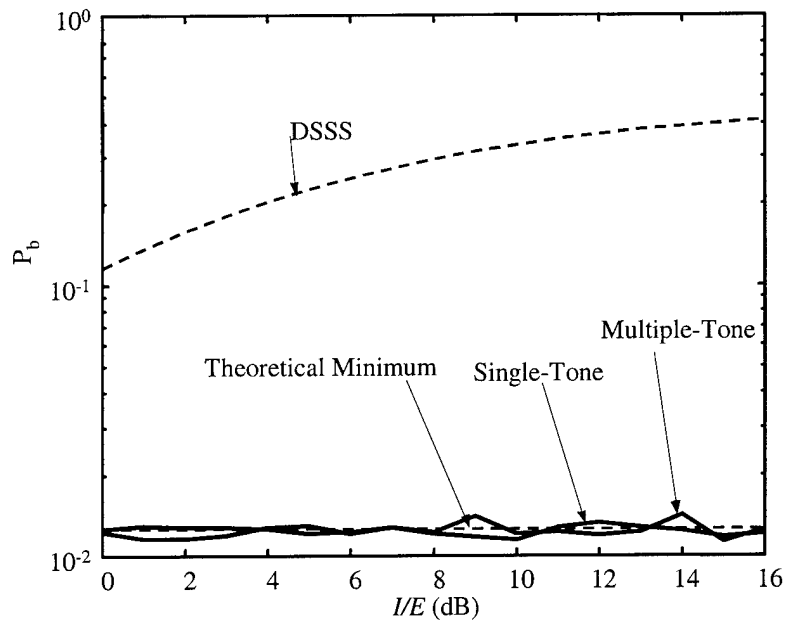
Figure 25. Single-Tone Interference: Antipodal Modulation with Spectral Shaping.
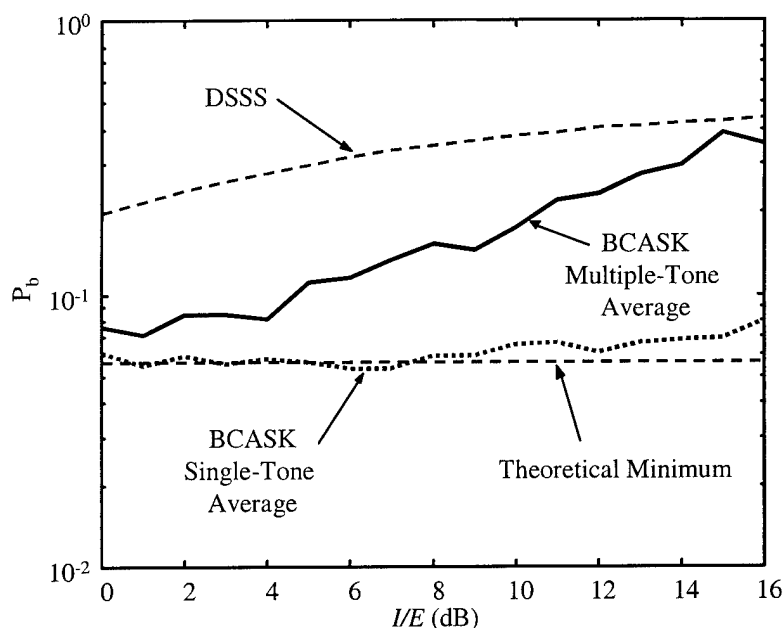
Figure 26. Single-Tone Interference: Orthogonal BCASK Modulation with Spectral Shaping.

4.4.3.3 Swept-Tone Interference – Spectral Shaping Employed

The final verification and validation scenario included the presence of swept-tone interference. In previous transform domain research, the swept-tone interference could not be accurately estimated due to the specific spectral estimation algorithm used [7]. Thus, performance improvements resulting from spectral shaping could not be investigated for the swept-tone interference.

As can be seen in Figure 27 and Figure 28, the WDCS avoids swept-tone interference for both the antipodal and orthogonal BCASK modulation schemes. At first glance, the apparent disconnect in P_b for I/E values between 7.0 and 8.0 dB is perhaps disconcerting and potentially leads one to believe the WDCS model is malfunctioning. However, after running several investigative simulations and thoroughly reviewing the data, it was discovered the apparent anomaly in the data is actually a result of WDCS thresholding and subband nulling process. Somewhere between I/E values of 7.0 and 8.0 dB (increasing interference power) the

interference power increases sufficiently such that one additional subband is nulled-out; reducing the interference effects and improving P_b as indicated in the figure.
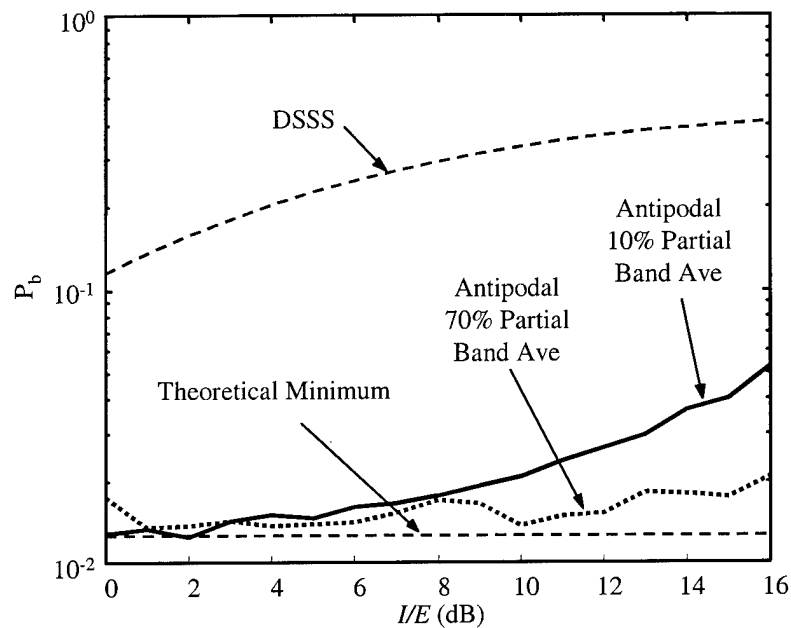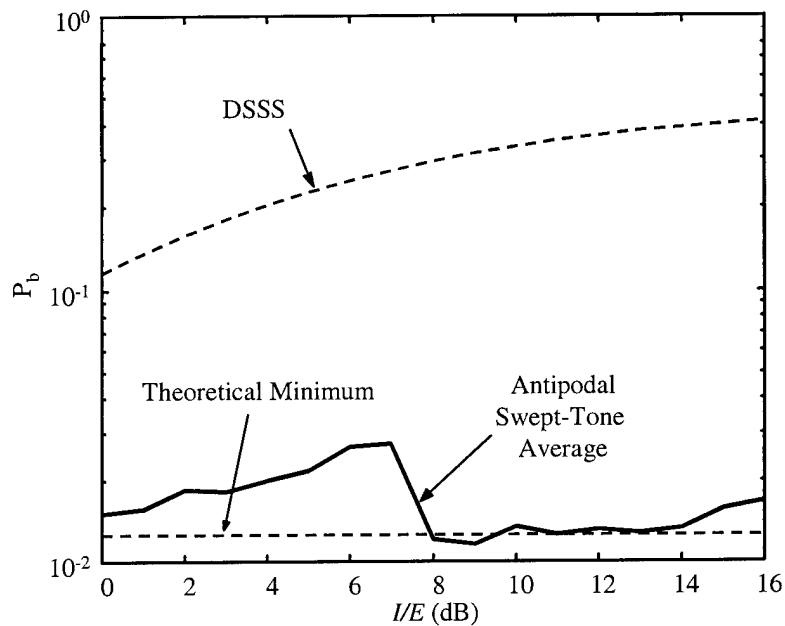

Figure 27. Swept-Tone Interference: Antipodal Modulation with Spectral Shaping.
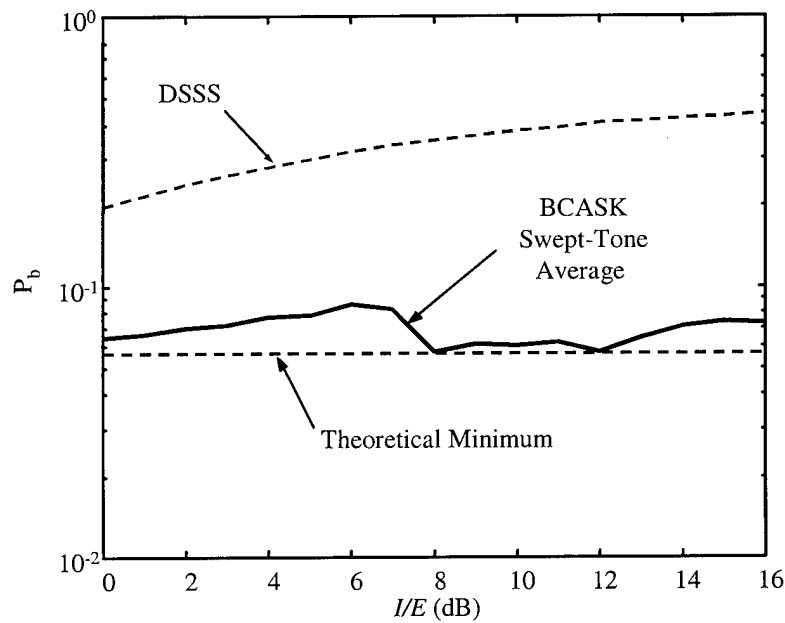
Figure 28. Swept-Tone Interference: Orthogonal BCASK Modulation with Spectral Shaping

4.5 Performance Increase

The data provided in previous sections demonstrates that the WDCS can successfully mitigate the effects of multiple types of interference. However, to compare WDCS interference avoidance capability with other systems, a metric is needed to quantify how much improvement the proposed WDCS offers. As defined in previous research and adopted for this analysis [7], an *improvement factor* $I(J_E)$ is used which represents a measure bit error performance improvement (decrease) provided by the WDCS relative to a another interference suppression/avoidance system. For this research, improvement is characterized relative to 1) a traditional DSSS using equivalent data modulation, and 2) a developmental Transform Domain Communication System (TDCS), all under identical scenarios. The *improvement factor* ratio $I(I_E)$ is defined as

$$I\left(I_E\right) = \frac{\left(P_b\right)_{Reference}}{\left(P_b\right)_{WDCS}} \tag{16}$$

where $I_E = I/E$, $(P_b)_{WDCS}$ is the WDCS probability of bit error for a given set of conditions, and $(P_b)_{Reference}$ is the reference system probability of bit error under identical conditions.

The WDCS bit error performance for all five interference scenarios of Section 4.3.3 were averaged together and compared to a traditional DSSS under similar conditions. The average WDCS bit error performance for the antipodal and orthogonal BCASK modulations is plotted in Figure 29 and Figure 30, respectively.
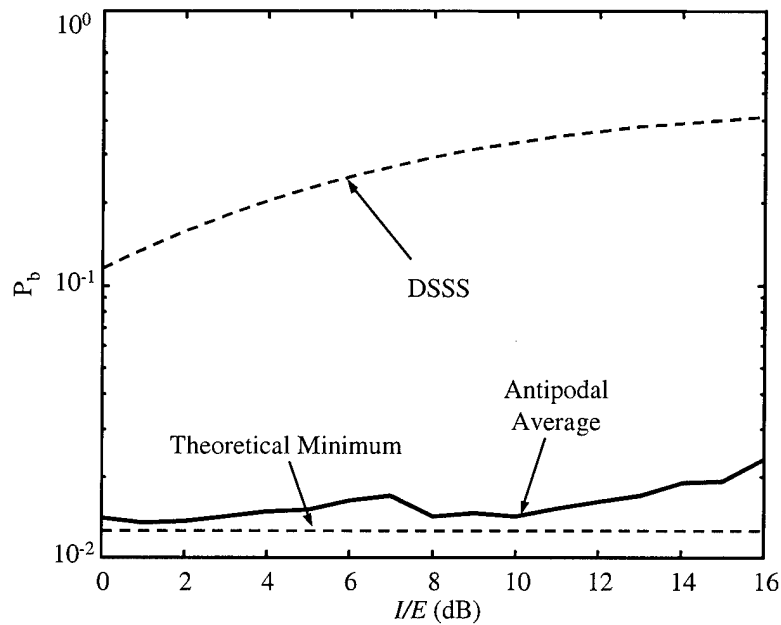
Figure 29. Average WDCS Bit Error Performance - Antipodal Data Modulation.
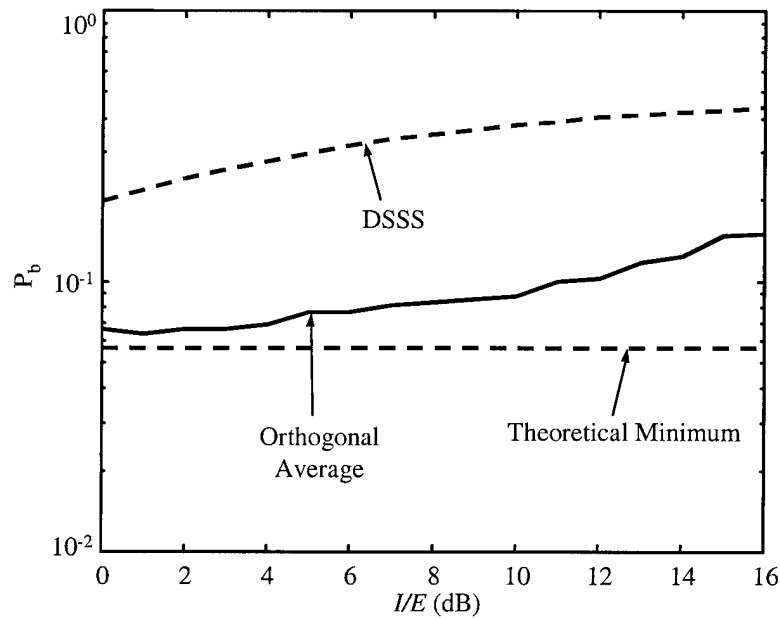
Figure 30. Average WDCS Bit Error Performance - Orthogonal Data Modulation.

From Figure 29, the average WDCS P_b using antipodal data modulation is approximately 1.6×10^{-2} over the range of I/E values considered, on average approximately 1 dB above the theoretical minimum value of 1.3×10^{-2}. The average WDCS improvement relative to an

46

equivalent DSSS system is 12.4 dB – approximately 0.4 dB poorer than the developmental TDCS-to-DSSS improvement [7].

From Figure 30, the average WDCS P_b using orthogonal data modulation is approximately 9.2×10^{-2} over the range of I/E values considered, on average approximately 1.8 dB above the theoretical minimum value of 5.7×10^{-2}. The average WDCS improvement relative to an equivalent DSSS system is 5.7 dB – approximately 1.1 dB poorer than the developmental TDCS-to-DSSS improvement [7].

However, it is unclear if the performance increases previously reported for the developmental TDCS included the multiple-tone and/or the swept-tone interference scenarios. If the multiple-tone interference scenario for the orthogonal modulation is disregarded (it had the poorest performance), then the average WDCS P_b using orthogonal data modulation is approximately 7.1×10^{-2} over the range of I/E values considered, on average approximately 0.9 dB above the theoretical minimum value of 5.7×10^{-2}. The average WDCS improvement relative to an equivalent DSSS system is 6.8 dB – approximately equal to the developmental TDCS-to-DSSS improvement [7]. Removing the multiple-tone interference in the antipodal modulation and the swept-tone interference in either modulation had no affect.

The overall difference in WDCS performance for the antipodal and orthogonal modulations is approximately 7.6 dB. The difference in performance with the multiple-tones remove is 6.5 dB. Theoretically, the difference between antipodal and orthogonal modulation is approximately 6.6 dB as indicated by comparing Equations (14) with (15).

4.6   Summary

This chapter provided modeling and simulation results for research conducted on a newly proposed wavelet domain communication system (WDCS). The concept of a basis function is

introduced and data presented that indicates the functions exhibit noise-like characteristics –
uniform phase distribution and cyclic orthogonality. Wavelet domain data of the interference
sources (single-tone, multiple-tone, swept-tone, and partial-band) is provided to present the
reader with a visual representation of how signal characteristics manifest themselves in the
wavelet domain – characteristics that are not intuitively obvious nor commonly seen in practice.
Simulation results for various interference scenarios were presented and used to characterize
WDCS interference avoiding capability – both the antipodal and orthogonal WDCS data
modulation schemes effectively improved the bit error performance in all interference scenarios
while outperforming an equivalent DSSS system. The proposed WDCS also performed on par
with a developmental transform domain communication system. In general, the bit error
performance improvement decreases as the I/E ratio is increased. In single-tone interference
cases, near theoretical minimum performance was achieved, independent of I/E. Under the
poorest conditions, the WDCS orthogonal data modulation technique outperformed the
traditional DSSS. An improvement factor was defined using a ratio of bit error performances,
WDCS-to-DSSS and WDCS-to-TDCS, and served as a basis for declaring the proposed WDCS a
viable, interference avoiding communication alternative. The relative improvement provided by
the WDCS is summarized in Table 1.

Table 1. Summary of Average WTDCS Improvement for E_b/N_o = 4.0 dB

	Antipodal Data Modulation	Orthogonal (BCASK) Data Modulation	WDCS/BCASK – No Multiple-Tone
Average P_b Above Theoretical Minimum	1dB	1.8 dB	0.9 dB
Average Improvement – Equivalent DSSS	12.4 dB	5.7 dB	6.8 dB
Average Improvement - Developmental TDCS	-0.4 dB	-1.1 dB	0.0 dB

CHAPTER 5

CONCLUSIONS AND RECOMMENDATIONS

5.1   Summary

A proposed wavelet domain communication system (WDCS) is shown to possess excellent interference avoidance capability in several different interference scenarios. The WDCS samples the electromagnetic environment and, using a wavelet-based transform implemented with a filter bank design, effectively determines the presence and time/scale location of interference. A time-domain communication signal (basis function) is then "designed" using wavelet domain information such that it contains minimal (ideally zero) energy in the interference region(s) – interference regions are detected and avoided through a thresholding and nulling operation. The resultant basis function is then data modulated prior to transmission. For perfect transmitter-receiver synchronization, the receiver generates an identical basis function for correlation with the received signal and subsequent data demodulation.

The proposed WDCS is modeled and simulation results generated using MATLAB®. Bit error performance is the primary metric used for analysis – WDCS performance is compared to 1) a traditional direct-sequence spread spectrum (DSSS) using binary phase shift keyed (BPSK) spreading modulation, and 2) a developmental transform domain communication system (TDCS) using a Fourier-based spectral estimation and basis function generation process. The WDCS performance is characterized using both antipodal and orthogonal forms of data modulation in scenarios containing single-tone, multiple-tone, swept-tone, and partial band interference.

5.2   Conclusions

Simulation results indicate the proposed WDCS offers a significant interference avoidance capability. Bit error performance analysis for several different interference scenarios reveals the WDCS system outperforms a traditional DSSS by a considerable margin and has comparable performance to the developmental TDCS considered, including the ability to properly estimate and mitigate swept-tone interference affects. The WDCS was simulated using an average signal bit energy-to-noise power spectral density (PSD) level (E_b/N_o) of 4.0 dB and average interference-to-average signal energy (I/E) levels ranging from 0.0 dB to 16.0 dB. An improvement metric was defined as the ratio of average the bit error performances, reference system over WDCS, taken over the range of I/E values considered. For antipodal data modulation, the average improvement was 12.4 dB, similar to the TDCS. Using binary orthogonal signal modulation, the average improvement was 5.7 dB, worse than TDCS. The WDCS did not outperform the TDCS in the simulated interference scenarios. However, the additional capability of avoiding the swept-tone interference outweighs the small difference in performance. For this reason, effort should be directed towards furthering the research on WDCS.

5.3   Recommendations for Future Research

This research demonstrated that the WDCS is a viable option for conducting interference avoidance communications. Given the limited scope of this effort, further areas of research are necessary to improve (perhaps optimize) the proposed WDCS design/implementation. These areas include, but are not limited to:

1. Implement spectral estimation using a wavelet-packet based decomposition technique.

2. Demonstrate *M*-Ary WDCS signaling capability.

3. Investigate using the WDCS as an intelligent interference source (smart jammer).

The first recommended area for continued research represents the next logical step into WDCS research. One of the problems associated with wavelet decomposition, as implemented for this research, is the non-uniform subband size – each subband contains a different number of samples, e.g., the first subband bin contains one-half the total number of samples, the next subband bin contains one-fourth the total number of samples, and so on. When the interference characteristics predominantly influence the largest bin, and the thresholding process subsequently causes this bin to be nulled-out, one-half of the available samples are set zero and are unavailable for constructing the communication symbols. The point at which this issue becomes problematic, and specific interference scenarios which perhaps cause it to occur, were not investigated under this research.

With packet-based wavelet decomposition, non-uniform bin size is no longer a problem. Wavelet packets themselves have the ability to decompose within each bin (perhaps optimally), effectively trading-off time resolution for scale resolution. This may seem like a problem, but with the current thresholding algorithm, time resolution isn't a factor. Using a packet-based wavelet decomposition, it is anticipated that the interference in some scenarios would be better localized, leaving more regions available for communication waveform generation.

The other ability of wavelet packets is optimal decomposition. Once a bin that is being decomposed no longer has significant interference energy, further processing does not have to be accomplished on that bin. By only processing those bins that contain interference energy, fewer calculations are performed, and processing time is saved. The less processing time needed, the more time that can be dedicated to observation or transmission.

The second recommendation for further research involves implementation of a WDCS using M-ary data modulation/signaling – the current effort only investigated binary signaling techniques. M-ary signaling involves using a set of M total communication symbols, versus the two used for binary signaling, which exhibit good (preferably orthogonal) correlation properties – strong autocorrelation and minimal cross-correlation (ideally zero) characteristics are desirable in communications to enhance symbol detection and estimation performance. Previous research on the developmental TDCS showed that the system was capable of being implemented with M-ary orthogonal signaling, as accomplished using a cyclic coded shift-keying (CCSK) technique. However, the WDCS results obtained here indicate the binary cyclic shift keying (BCSK) performance is not indicative of an orthogonal modulation; although not investigated, it is unlikely that the orthogonal M-ary CSK modulation techniques will work satisfactorily with the proposed WDCS. Therefore, different M-ary modulation methods need to be investigated to expand WDCS capability to multiple dimensions.

The last recommended area of research abandons the idea of using a WDCS (a misnomer in this case) for communicating, rather, it considers using the WDCS as an intelligent interference source. Given that the WDCS has the inherent ability to sample the environment and determine signal presence, if such a system could ascertain what frequencies are in use by friendly forces, it could design a specific interference waveform to selectively interfere with other, perhaps hostile, signals in the environment. Alternately, the WDCS could generate a wideband (barrage) interference waveform with energy only in the regions containing signals to be intentionally interfered with – this effectively increases jamming efficiency since the available interference energy is only dispersed in regions where systems are operating, while avoiding fratricide.

5.4 Technical Contributions

The following technical conference papers are a result of this research:

1. MILCOM 2001 – Submitted

   Wavelet Domain Communication System (WDCS) Interference Avoidance Capability: Analytic, Modeling and Simulation Results

2. SCI 2001 - Submitted

   Performance Characterization of a Proposed Wavelet Domain Communication System (WDCS)

3. GLOBECOM 2001 – In-Progress

```
function [proberr,toterr] = master(eb_no,numerr,jamtype,jamwid,fj,N)
%  [proberr,toterr] = master(eb_no,numerr,jamtype,jamwid,fj,N)
%
%  eb_no - in dB
%  numerr - number of errors to collect
%  jamtype,jamwid,fj - variables in create_noise.m
%  N - length of bit
%
%
% eb_no is the eb/no ratio in dB
% ******assumes no is 1 ******

% Sets up different realizations of random variables
rand('seed',sum(100*clock));
randn('seed',sum(100*clock));


%%%%%%%%%%%%%%%%%%%%%%%%%%%%%%%%%%%%%%%%%%%%%%%%%%%%%%%%%%%%%%%%
%      Parameters
%
L =100;                % number of data bits
numje=1;               % number of eb/nos
jam=0;                 % jammer status (1 = on, 0 = off)
%%%%%%%%%%%%%%%%%%%%%%%%%%%%%%%%%%%%%%%%%%%%%%%%%%%%%%%%%%%%%%%%



%  generate PN phase code
np = 8;                % # phase points on unit circle
pn_deg = 11;           % deg of generator poly
pn_poly = 4005;        % octal representation of generator poly
pn_fill = 5777;        % octal representation of fill poly
phase_code = pr_phase(N, np, pn_deg, pn_poly, pn_fill);

% determine spectrum from spectral sample

% define J/E
JE = 0:1:20;

%initial temp variables
toterr = 0;
proberr = 0;
count1 = 1;


while count1<(numje+1)
   if jam == 0
      sigmaj_sqrd = 0;
   else
      sigmaj_sqrd = invdb(JE(1,count1))*invdb(eb_no);


   end
```

```
%initialize variables
g=ones(1,N);
Ns=log2(N);

% Wavelet Filter
h=daub(8);

sigma_sqrd = 1;   %  noise variance

% Create interference
[na,ja,sampa]=create_noise(sigma_sqrd,sigmaj_sqrd,jamwid,fj,N,L,jamtype);

% If no interference other than AWGN, no thresholding
if cov(sampa) > 1.2*sigma_sqrd
    gg = dwt(sampa,h,Ns);
    g=dwt_thresh3(sampa,h,Ns);
end

Hint = g;  % All ones from above
disp('No noise')

% If every coefficient is nulled out, then an all 1's is transmitted and
an error reported
if max(g)==0;
    g = ones(1,N);
    disp('error')
end

% Energy Scaling
a = sum(abs(Hint).^2);
A = sqrt(invdb(eb_no)/a);
H = A*Hint;

% Phase Encoding
C_freq = H.*phase_code;

% Basis Function Creation
icode = idwt(C_freq,h,Ns);

% Symbol Creation
c1 = icode;   %symbol 1
c2 = [-c1(ceil(end/2):end) c1(1:ceil(end/2)-1)];   % BCASK
%c2 = -icode; %Antipodal

% start Bernoulli trials
count=0;
errors=0;
while errors < numerr

    %  fill data vector
    data = round(rand(1,L));

    %  generate signal vector for xmsn
    sint1 = find(data);
    sint2 = find(data == 0);
```

```matlab
        sinta = zeros(1,length(data));
        sintb = zeros(1,length(data));
        sinta(sint1)=ones(1,length(sint1));
        sintb(sint2)=ones(1,length(sint2));

        s1a = conj(c1')*sinta;
        s2a = conj(c2')*sintb;
        s = reshape(s1a+s2a,1,L*N);



        %  generate different realization of noise and jamming vector

[nt,jt,sampt]=create_noise(sigma_sqrd,sigmaj_sqrd,jamwid,fj,N,L,jamtype);
        if jam == 0
            sampt = nt;
        end

        %  generate rcvd vector
        x = s + sampt;
        % correlate with c1
        c1ref=reshape(conj(c1')*ones(1,L),1,L*N);
        Ztest1=x.*conj(c1ref);
        Ztv1=reshape(Ztest1,N,L);
        Zt1=sum(Ztv1)/(invdb(eb_no));

        % correlate with c2
        c2ref=reshape(conj(c2')*ones(1,L),1,L*N);
        Ztest2=x.*conj(c2ref);
        Ztv2=reshape(Ztest2,N,L);
        Zt2=sum(Ztv2)/(invdb(eb_no));

        s0 = find(real(Zt1)>=real(Zt2));
        output=zeros(1,length(data));
        output(s0)=ones(1,length(s0));

        % determine Pb
        errors = errors + length(find(data-output))

        count = count + 1;

    end

    toterr(1,count1) = errors;
    proberr(1,count1) = toterr(1,count1)/(L*count);

    count1=count1 + 1;
end
```

APPENDIX B – Interference Code

```
function [n0,j3s,samp] = create_noise(sigma_sqrd,sigmaj_sqrd,...
   jamwid,fj,nsamps,L,jamtype)

% function [n0,j3s,samp] = create_noise(sigma_sqrd,sigmaj_sqrd,...
%    jamwid,fj,nsamps,jamtype)
%
% create_noise.m creates a noisy environment by adding AWGN
% with a jamming signal.
%
% Inputs: sigma_sqrd  - noise variance
%         sigmaj_sqrd - jammer variance
%         jamwid      - jammer width (rho) - for partial band jammer
%         fj          - jammer freuency - for tone jammer
%         nsamps      - number of samples from environment per bit period
%         L           - number of bit periods to sample
%         jamtype     - 1 = partial band jammer, 2 = tone jammer, 3 = swetp
% tone, 4 = multiple tone
%
% Outputs: n0         - AWGN
%          j3s        - jamming signal
%          samp       - environment
%
% Code originally written by Capt Radcliffe in 1996.
% Function written and code modified in October 1999 by Capt Marcus Roberts.
% Modified in September 2000 by Lt Randy Klein

rand('state',sum(100*clock));
randn('state',sum(100*clock));

% Create AWGN
n0i = (1/sqrt(2))*sqrt(sigma_sqrd)*randn(1,nsamps*L);
n0q = (1/sqrt(2))*sqrt(sigma_sqrd)*randn(1,nsamps*L);
n0 = n0i + i*n0q;     % in-phase and quadrature noise

% Create additional interference (jammer)
N = nsamps;
if jamtype == 1 % Partial band jammer
   fu = ceil(fj + (jamwid/2)*N/2);
   fl = floor(fj - (jamwid/2)*N/2);
   numzs = (fu - fl)*L;
   if fu > N/2
      error('Alias high')
   elseif fl < 1
      error('Alias low')
   end

   j0is = (2/sqrt(2))*sqrt(sigmaj_sqrd)*randn(1,N*L);
   j0qs = (2/sqrt(2))*sqrt(sigmaj_sqrd)*randn(1,N*L);
   parfils = zeros(1,N*L);
   parfils(fl*L:fu*L-1) = ones(1,numzs);
   parfils = parfils/sqrt(jamwid);
   J3is = fft(j0is);
   J3qs = fft(j0qs);
```

```matlab
    J3iints = J3is.*parfils;
    J3qints = J3qs.*parfils;
    j3is = real(ifft(J3iints));
    j3qs = real(ifft(J3qints));
    j3s = j3is + i*j3qs;

elseif jamtype == 2 % Tone jammer
    if fj > N/2
        error('Alias high')
    end
    ns = 0:N*L-1;
    phis = 2*pi*rand(1);
    j3s = sqrt(sigmaj_sqrd)*exp(i*(2*pi*fj*ns/N + phis));

elseif jamtype == 3 %swept tone

    b=5;   %number of bits jammer sweeps
    t=0:1/N:b-1/N;
    x=L/b;
    p=1;
    f=nsamps/2*.6;   % .6 is amount of bandwidth jammer sweeps

    f1=nsamps/4+f/2;   % highs and lows of sweeps
    f0=nsamps/4-f/2;

    beta = (f1-f0).*(b.^(-p));
    if fj > N/2
        error('Alias high')
    end

    phi = 2*pi*rand(1);

    j = sqrt(sigmaj_sqrd)*exp(i*2*pi * ( beta./(1+p).*(t.^(1+p)) + f0.*t +
phi));

    j3s = [];
    for z=1:x
        j3s=[j3s j];
    end



elseif jamtype == 4 %multiple tone
    if 1.5*fj > N/2
        error('Alias High')
    elseif .5*fj < 1
        error('Alias Low')
    end

    numtones = 7;   %number of tones
    BW = nsamps/2;
    fj = BW/(numtones+1);
    f=fj;
    ns = 1:N*L;
    phis = 2*pi*rand(1);
    j3s = 0;
    for k = 1:numtones
```

```
        j = sqrt(sigmaj_sqrd/numtones)*exp(i*(2*pi*fj*(ns-1)/N + phis));
        j3s = j+j3s;
        fj=fj+f;
    end

end

samp = j3s+n0;
```

APPENDIX C - Wavelet Transform and Thresholding Code

```
function g = dwt_threshold(f,h,NJ)
% function g = dwt(f,h,NJ)  Calculates the DWT of periodic f
% with scaling filter h and NJ scales
% Reference: Burrus, Gopiath, Guo.  Introduction to Wavelets
% and Wavelet Transforms: A Primer. New Jersey, Prentice Hall
% 1998.  p. 263
%
% Modified by Randy Klein, 2000.

N=length(h);
Lf=length(f);
c=f;
t=[];
x = zeros(1,NJ+1);

%Determine power of incoming signal
L2 = sum(abs(f).^2)/Lf;  %L2 metric
L2_n = 1;
L2_R = L2/L2_n;


%Determines number of scales if none provided in input
if isempty(NJ)
    NJ = round(log10(Lf)/log10(2));
end

%Scaling Filter
h0 = fliplr(h);

%Wavelet Filter
h1 = h;
h1(1:2:N) = -h1(1:2:N);

%Mallat's Algorithm
for j=1:NJ
    Lc = length(c);

    %Make periodic
    c = [c(mod((-(N-1):-1),Lc)+1) c];

    %Convolve and down sample
    d = conv(c,h1);
    d = d(N:2:(N+Lc-2));
    c = conv(c,h0);
    c = c(N:2:(N+Lc-2));

    % Threshold Bands
    Nd = length(d);
    L2_s = sum(abs(d).^2)/Nd;
    if L2_s < 1.2  % Compares power in band to noise power of 1
        x(j) = 1;
    end
```

```
    %Concatenate wavelet coefficients
    t = [d,t];

end
d=c;

% Threshold Bands, same as before but for coarse coeff
Nd = length(d);
L2_s = sum(abs(d).^2)/Nd;

if L2_s < 1.2
    x(j+1) = 1;
end

%The DWT
y = 0;
z = [];
for j = 1:NJ
    if x(j) == 1;
        y = ones(1,(2^(NJ+1-j))/2);
    else
        y = zeros(1,(2^(NJ+1-j))/2);
    end
    z = [y z];
end
if x(NJ+1) == 1
    y = 1;
else
    y = 0;
end
z = [y z];

g = z;
```

APPENDIX D – Mother Wavelet Code

```
function hn=daub(N)
% hn=daub(N)
% Function to compute the Daubechies scaling coefficients from
% her development in the paper, "Orthonormal bases of compactly
% supported wavelets", CPAM, Nov. 1988 page 977, or in her book
% "Ten Lectures on Wavelets", SIAM, 1992 pages 168, 216.
% The polynomial R in the reference is set to zero and the
% minimum phase factorization is used.
% Not accurate for N > 20.  Check results for long h(n).
% Input:  N is length of filter.
% Output: hn = h(n) length-N min phase scaling fn coeffs
%
% Reference: Burrus, Gopiath, Guo.  Introduction to Wavelets
% and Wavelet Transforms: A Primer. New Jersey, Prentice Hall
% 1998.  p. 260


%Initialize variables
a = 1;
p = 1;
q = 1;
N2=N/2;

%Initialize factors of zeros at -1
hn = [1 1];

for j = 1:N2-1

    %Generate polynomial for zeros at -1
    hn = conv(hn,[1,1]);

    %Generate the binomial coeff. of L
    a = -a*0.25*(j+N2-1)/j;

    %Generate variable values of L
    p = conv(p,[1,-2,1]);

    %Combine terms for L
    q = [0 q 0] + a*p;
end

%Factor L
q = sort(roots(q));

%Combine zeros at -1 and L
hn = conv(hn,real(poly(q(1:N2-1))));

%Normalize
hn = hn*sqrt(2)/(sum(hn)
```

APPENDIX E – PR Phase Code / Mapping

```
function [phs] = pr_phase(N,np,reg,taps,fill);
% [phs] = pr_phase(N,np,reg,taps,fill);
%
% N = number of points in the waveform
% np = number of phase points in the phase plane
% reg = register length for the pn code generator
% taps = taps for the pn code generator
% fill = initial fill for the pn code generator
%
% requires the pn.m function
%
% Returns a complex vector of phases

bits = ceil(log2(np));

% Edited by Patrick Swackhammer, 9 Sep 98
%chips = pn(reg,taps,fill,N*bits,1,1);
chipsVec = pn(reg,taps,fill,N,1,1);
chips = chipsVec;
for i = 1:(bits-1)
    chips = [chips; chipsVec];
end

% Edited by Patrick Swackhammer, 9 Sep 98
%phs = reshape(chips,bits,N);
phs = matshift(chips);

%phs = 2.^[0:bits-1]*phs*2*pi/np;
phs = 2.^[bits-1:-1:0]*phs*2*pi/np;
phs = exp(j*phs);

return;
```

APPENDIX F – Inverse Wavelet Transform

```
function f = idwt(g,h,NJ)
% function f = idwt(g,h,NJ)  Calculates the IDWT of periodic f
% with scaling filter h and NJ scales
% Reference: Burrus, Gopiath, Guo.  Introduction to Wavelets
% and Wavelet Transforms: A Primer. New Jersey, Prentice Hall
% 1998.  p. 263
%

N = length(h);
L = length(g);

%Determines number of scales if none provided in input
if isempty(NJ)
   NJ = round(log10(L)/log10(2));
end

%Scaling Filter
h0 = h;

%Wavelet Filter
h1 = fliplr(h);
h1(2:2:N) = -h1(2:2:N);
LJ = L/(2^NJ);
c = g(1:LJ);

%Mallat's Algorithm
for j = 1:NJ

   %Make periodic
   w = mod(0:N/2-1,LJ)+1;

   %Wavelet Coeffs
   d = g(LJ+1:2*LJ);

   %Up sample & periodic
   cu(1:2:2*LJ+N) = [c c(1,w)];
   du(1:2:2*LJ+N) = [d d(1,w)];

   %Convolve and combine
   c = conv(cu,h0) + conv(du,h1);
   c = c(N:N+2*LJ-1);

   %Periodic part
   LJ = 2*LJ;

end

%The IDWT
f = c;
```

BIBLIOGRAPHY

[1]   Andren, Carl F., et. al. <u>Low Probability-of-Intercept Communication System</u>. Harris Corporation, U.S. Patent 5 029 184, 1991.

[2]   Burrus, C. Sidney, et. Al. <u>Introduction to Wavelets and Wavelet Transforms: A Primer</u>. New Jersey: Prentice Hall, 1998.

[3]   German, Edgar H. "Transform Domain Signal Processing Study Final Report." Technical Report, Reistertown MD: Contract: Air Force F30602-86-C-0133, August 1988.

[4]   Milstein, Arsenault, Das. "Transform Domain Processing for Digital Communications Systems Using Surface Acoustic Wave Devices." Technical Report, Troy, NY: Contract: Army DAAG-29-77-G-0205, May 1978.

[5]   Milstein, Arsenault, Das. "Processing Gain Advantage of Transform Domain Filtering DS – Spread Spectrum Systems." <u>MILCOM '82</u>, October 1982.

[6]   Peterson, Roger L., et. al. <u>Introduction to Spread Spectrum Communications</u>. New Jersey: Prentice Hall, 1995.

[7]   Radcliffe, Rodney A. <u>Design and Simulation of a Transform Domain Communication System</u>. MS Thesis, AFIT/GE/ENG/96D-16, Air Force Institute of Technology, Wright-Patterson AFB OH, December 1996.

[8]   Radcliffe, Rodney A. and Gerald C. Gerace. "Design and Simulation of a Transform Domain Communication System." <u>MILCOM '97</u>, October 1997.

[9]   Roberts, Marcus L. <u>Synchronization of a Transform Domain Communication System</u>. MS Thesis, AFIT/GE/ENG/00M-15, Air Force Institute of Technology, Wright-Patterson AFB OH, March 2000.

[10]   Sklar, Bernard. <u>Digital Communications: Fundamentals and Applications</u>. New Jersey: Prentice Hall, 1988.

[11]   Stremler, Ferrel G. <u>Introduction to Communication Systems: Third Edition</u>. Reading MA: Addison-Wesley, 1990.

[12]   Swackhammer, Patrick J. <u>Design and Simulation of a Multiple Access Transform Domain Communication System</u>. MS Thesis, AFIT /GE/ENG/99M-28, Air Force Institute of Technology, Wright-Patterson AFB OH, March 1999.

VITA

Lieutenant Randall Wayne Klein was born   in Santa Monica, CA. In June 1995,

he graduated from Larry A. Ryle High School in Union, KY. He entered the United

States Air Force Academy and graduated with a Bachelor of Science in Electrical

Engineering on 2 June, 1999. While at the Air Force Academy, he earned academic

distinction by graduating in the top 10% of his class academically. In August 1999, he

entered the Air Force Institute of Technology (AFIT) Master's program at Wright-

Patterson AFB, OH. As a Master's candidate, in the Department of Electrical and

Computer Engineering at AFIT, his focus of study was on communications and computer

networks. He is a member of Tau Beta Pi. Upon graduation, he will be assigned to the

National Air Intelligence Center (NAIC) at Wright-Patterson AFB, OH.

REPORT DOCUMENTATION PAGE		*Form Approved* *OMB No. 0704-0188*

The public reporting burden for this collection of information is estimated to average 1 hour per response, including the time for reviewing instructions, searching existing data sources, gathering and maintaining the data needed, and completing and reviewing the collection of information. Send comments regarding this burden estimate or any other aspect of this collection of information, including suggestions for reducing the burden, to Department of Defense, Washington Headquarters Services, Directorate for Information Operations and Reports (0704-0188), 1215 Jefferson Davis Highway, Suite 1204, Arlington, VA 22202-4302. Respondents should be aware that notwithstanding any other provision of law, no person shall be subject to any penalty for failing to comply with a collection of information if it does not display a currently valid OMB control number.
PLEASE DO NOT RETURN YOUR FORM TO THE ABOVE ADDRESS.

1. REPORT DATE *(DD-MM-YYYY)* March 2001	2. REPORT TYPE Master's Thesis	3. DATES COVERED *(From - To)*

4. TITLE AND SUBTITLE WAVELET DOMAIN COMMUNICATION SYSTEM (WDCS): DESIGN, MODEL, SIMULATION, AND ANALYSIS	5a. CONTRACT NUMBER
	5b. GRANT NUMBER
	5c. PROGRAM ELEMENT NUMBER
6. AUTHOR(S) Klein, Randall W., Lieutenant, USAF	5d. PROJECT NUMBER
	5e. TASK NUMBER
	5f. WORK UNIT NUMBER

7. PERFORMING ORGANIZATION NAME(S) AND ADDRESS(ES) Air Force Institute of Technology Graduate School of Engineering and Management (AFIT/EN) 2950 P Street, Building 640 WPAFB OH 45433-7765	8. PERFORMING ORGANIZATION REPORT NUMBER AFIT/GE/ENG/01M-16

9. SPONSORING/MONITORING AGENCY NAME(S) AND ADDRESS(ES) Attn: James P. Stephens AFRL/SNRW WPAFB OH 45433 DSN: 785-5579 x4239 james.stephens@wpafb.af.mil	10. SPONSOR/MONITOR'S ACRONYM(S)
	11. SPONSOR/MONITOR'S REPORT NUMBER(S)

12. DISTRIBUTION/AVAILABILITY STATEMENT
APPROVED FOR PUBLIC RELEASE
DISTRIBUTION UNLIMITED

13. SUPPLEMENTARY NOTES
AFIT Technical POC: Michael A. Temple, AFIT/ENG
michael.temple@afit.edu

14. ABSTRACT
A proposed wavelet domain communication system (WDCS) using transform domain processing is demonstrated as having enhanced interference avoidance capability under adverse environmental conditions. The proposed system is modeled and simulation results are obtained using MATLAB. Relative to an equivalent DSSS, the WDCS provided bit error performance improvement in several different interference scenarios. The system also demonstrated comparable performance to a developmental TDCS while providing significant improvement in scenarios containing swept-tone interference. The system was evaluated using a signal bit energy-to-noise power level (Eb/No) of 4.0 dB and interference energy-to-signal energy (I/E) ratios ranging from 0 dB to 16.0 dB. As defined, performance improvement metrics representing the ratio of DSSS-to-WDCS and DSSS-to-TDCS bit error rates were used for characterizing performance. For antipodal data modulation, the average (over all interference scenarios) DSSS-to-WDCS performance improvement was 12.4 dB, approximately equal to the DSSS-to-TDCS (comparable performance). For binary orthogonal data modulation, the average DSSS-to-WDCS improvement was 5.7 dB vs. 6.8 dB for the DSSS-to-TDCS comparison. These results indicate the proposed WDCS is a viable option for interference avoidance

15. SUBJECT TERMS
Wavelet Domain Communication, Transform Domain Processing, Interference Avoidance, Binary Cyclic Antipodal Shift Keying

16. SECURITY CLASSIFICATION OF:			17. LIMITATION OF ABSTRACT	18. NUMBER OF PAGES	19a. NAME OF RESPONSIBLE PERSON Dr. Michael A. Temple, AFIT/ENG
a. REPORT U	b. ABSTRACT U	c. THIS PAGE U	UU	79	19b. TELEPHONE NUMBER *(Include area code)* (937) 255-3636, ext 4703

Standard Form 298 (Rev. 8/98)
Prescribed by ANSI Std. Z39.18